JOURNAL OF GEOPHYSICAL RESEARCH, VOL. 103, NO. B12, PAGES 30,205–30,229, DECEMBER 10, 1998

Time variability of the Earth's gravity field: Hydrological and oceanic effects and their possible detection using GRACE

John Wahr and Mery Molenaar

Department of Physics and Cooperative Institute for Research in Environmental Science, University of Colorado, Boulder

Frank Bryan

National Center for Atmospheric Research, Boulder, Colorado

Abstract. The GRACE satellite mission, scheduled for launch in 2001, is designed to map out the Earth's gravity field to high accuracy every 2-4 weeks over a nominal lifetime of 5 years. Changes in the gravity field are caused by the redistribution of mass within the Earth and on or above its surface. GRACE will thus be able to constrain processes that involve mass redistribution. In this paper we use output from hydrological, oceanographic, and atmospheric models to estimate the variability in the gravity field (i.e., in the geoid) due to those sources. We develop a method for constructing surface mass estimates from the GRACE gravity coefficients. We show the results of simulations, where we use synthetic GRACE gravity data, constructed by combining estimated geophysical signals and simulated GRACE measurement errors, to attempt to recover hydrological and oceanographic signals. We show that GRACE may be able to recover changes in continental water storage and in seafloor pressure, at scales of a few hundred kilometers and larger and at timescales of a few weeks and longer, with accuracies approaching 2 mm in water thickness over land, and 0.1 mbar or better in seafloor pressure.

1. Introduction

For the past few decades, the tracking of artificial satellites in Earth orbit has been the principal means of determining the Earth's gravity field at global to regional scales. Because the orbital motion of a satellite is largely determined by gravitational forces, orbit solutions based on precise satellite tracking observations can be used to invert for the gravity field. So far, the most useful satellites for this purpose have been those that use ground-based lasers to measure the Earth-satellite distance. And the most useful of those has been LAGEOS, launched in 1976 to an altitude of about 6000-km and still providing range measurements of the highest quality.

High-altitude satellites like LAGEOS, however, can provide useful gravity information only at relatively long wavelengths. The most recent satellite-only global gravity model, JGM-3 [*Tapley et al.*, 1996], includes spherical harmonic coefficients out to degree and order 70, which corresponds to half-wavelengths of 285 km and larger. Shorter-wavelength terms decay rapidly with distance above the Earth's surface, so that their accurate detection would require a low-altitude satellite. Low-altitude satellites, however, are subject to considerably larger nongravitational forces, primarily from the atmosphere, and these can greatly degrade the gravity inversions at all wavelengths. The 6000-km altitude of LAGEOS is a reasonable compromise between a low enough orbit to provide good resolution, and yet a high enough orbit to minimize atmospheric drag effects.

The satellite laser ranging measurements have also been used to detect temporal variations in the Earth's gravity field. The gravity field depends on the Earth's mass distribution, which can undergo changes due to dynamic processes within the Earth and on and above its surface. Laser ranging to LAGEOS and other satellites has provided information about seasonal, decadal, and secular changes in a few (from two to about five, depending on the analysis) of the very largest-scale, zonal components of the gravity field [see, e.g., *Yoder et al.*, 1983; *Rubincam*, 1984; *Cheng et al.*, 1989; *Gegout and Cazenave*, 1993; *Eanes, 1995*; *Nerem et al.*, 1993; *Dong et al.*, 1996]. The sources of this variability have been proposed as including mass redistribution in the atmosphere (for the seasonal terms), the 18.6-year gravitational tide in the solid Earth and oceans (for the decadal variability), and a combination of postglacial rebound

Paper number 98JB02844.
0148-0227/98/98JB-02844$09.00

and changing Antarctic and Greenland ice volumes (for the secular terms). More detailed interpretations have been prevented by the fact that so few temporally varying components have been identified.

Gravity field solutions should improve dramatically with the launch of GRACE, a dedicated-gravity satellite mission under the joint sponsorship of NASA and the Deutsches Zentrum fur Luft und Raumfahrt, and presently scheduled for launch in 2001 with a nominal 5-year lifetime. GRACE will consist of two satellites in low-Earth orbit (an initial altitude in the range of 450-500 km) and a few hundred kilometers apart, that range to each other using microwave phase measurements. Onboard GPS receivers will determine the position of each spacecraft in a geocentric reference frame. Onboard accelerometers will be used to detect the nongravitational acceleration so that its effects can be removed from the satellite-to-satellite distance measurements. The residuals will be used to infer the gravitational acceleration and thus to map the gravity field. Because the satellites are in such low orbit, the gravity field will be determined orders of magnitude more accurately, and to considerably higher resolution, by GRACE than by any other existing satellite. This will not only result in better maps of the Earth's static gravity field but will also permit temporal variations in gravity to be determined down to scales of a couple hundred kilometers and shorter every 2-4 weeks. These temporal variations can be used to study a large variety of problems in a number of disciplines, from monitoring changes in water and snow storage on continents, to determining variability in seafloor pressure, to measuring the redistribution of ice and snow on the polar ice caps, to constraining postglacial rebound deformation within the solid Earth. A complete description of these and other applications of satellite measurements of temporal changes in gravity is given by *Dickey et al.* [1997].

The main purpose of our paper is to describe the possible hydrological and oceanographic contributions to time-dependent gravity and to anticipate the accuracy with which GRACE observations can recover those effects. We address three problems in this paper. The first is to characterize the likely hydrological, oceanographic, and atmospheric contributions to time-dependent gravity in terms of amplitudes and of temporal and spatial scales. The second is to describe a possible method for using the gravity information from GRACE to infer changes in surface mass. The third is to estimate the accuracy with which GRACE can estimate those surface mass changes.

2. Preliminaries

In this paper we will use estimates of surface mass variability to compute gravity signals, and we will use simulated GRACE gravity data to recover surface mass variability. For both types of applications we will use equations that relate changes in surface mass to changes in gravity. Those equations are described in this section. We also discuss here the geophysical data sets used below to estimate the time-dependent gravity signal.

2.1. Equations Relating Surface Mass to Gravity

The Earth's global gravity field is commonly described in terms of the shape of the geoid: the equipotential surface corresponding to mean sea level over the oceans. It is usual to expand the geoid shape N as a sum of spherical harmonics [see, e.g., *Chao and Gross*, 1987]

$$N(\theta,\phi) = a\sum_{l=0}^{\infty}\sum_{m=0}^{l}\tilde{P}_{lm}(\cos\theta)(C_{lm}\cos(m\phi) + S_{lm}\sin(m\phi)) \quad (1)$$

where a is the radius of the Earth, θ and ϕ are colatitude and east longitude, C_{lm} and S_{lm} are dimensionless coefficients, and the $\tilde{P}_{lm}$ are normalized associated Legendre functions:

$$\tilde{P}_{lm}(x) = \sqrt{(2-\delta_{m0})(2l+1)\frac{(l-m)!}{(l+m)!}} \times \frac{(1-x^2)^{\frac{m}{2}}}{2^l l!}\frac{d^{l+m}}{dx^{l+m}}(x^2-1)^l \quad (2)$$

A satellite geoid model typically consists of numerical values for the C_{lm} and S_{lm} variables. GRACE, for example, will probably deliver C_{lm} and S_{lm} variables complete to degree and order (i.e., l and m) of about 100 every few weeks.

Suppose there is a time-dependent change in the geoid ΔN. You could imagine ΔN as representing either the change in N from one time to another, or as the difference between N at one time and a time average of N, or as some other representation of a changing N. This change in N can be represented in terms of changes, ΔC_{lm} and ΔS_{lm}, in the spherical harmonic geoid coefficients as

$$\Delta N(\theta,\phi) = a\sum_{l=0}^{\infty}\sum_{m=0}^{l}\tilde{P}_{lm}(\cos\theta)(\Delta C_{lm}\cos(m\phi) + \Delta S_{lm}\sin(m\phi)) \quad (3)$$

Let $\Delta\rho(r,\theta,\phi)$ be the density redistribution causing this geoid change. By combining equations (3), (7), and (9)-(11) of *Chao and Gross* [1987]: it can be shown that

$$\left\{\begin{array}{c}\Delta C_{lm}\\ \Delta S_{lm}\end{array}\right\} = \frac{3}{4\pi a\rho_{\text{ave}}(2l+1)}\int \Delta\rho(r,\theta,\phi)\,\tilde{P}_{lm}(\cos\theta) \times\left(\frac{r}{a}\right)^{l+2}\left\{\begin{array}{c}\cos(m\phi)\\ \sin(m\phi)\end{array}\right\}\sin\theta\,d\theta\,d\phi\,dr \quad (4)$$

where ρ_{ave} is the average density of the Earth (= 5517 kg/m^3).

Suppose $\Delta\rho$ is concentrated in a thin layer of thickness H at the Earth's surface. For our applications, this layer must be thick enough to include those portions of the atmosphere, oceans, ice caps, and below-ground water storage with significant mass fluctuations. Thus H is mostly determined by the thickness of the atmosphere and is of the order of 10-15 km.

We define the change in surface density (i.e., mass/area), $\Delta\sigma$, as the radial integral of $\Delta\rho$ through this layer:

$$\Delta\sigma(\theta,\phi) = \int_{\text{thin layer}} \Delta\rho(r,\theta,\phi)dr \qquad (5)$$

The GRACE errors for large values of l are likely to be large enough that there is little hope of GRACE recovering useful time variable geoid coefficients for $l > \approx 100$. In fact, most of the recoverable time-dependent gravity signal will be concentrated at degrees well below 80 or so. Thus the sum over (l,m) in (3) can be truncated to degrees $l < l_{\max}$, where, at most, $l_{\max} \approx 100$. Suppose H is thin enough that $(l_{\max}+2)H/a << 1$. Then, $(r/a)^{l+2} \approx 1$, and so (4) reduces to

$$\left\{ \begin{array}{c} \Delta C_{lm} \\ \Delta S_{lm} \end{array} \right\}_{\text{surf mass}} = \frac{3}{4\pi a \rho_{\text{ave}}(2l+1)} \int \Delta\sigma(\theta,\phi) \times \tilde{P}_{lm}(\cos\theta) \left\{ \begin{array}{c} \cos(m\phi) \\ \sin(m\phi) \end{array} \right\} \sin\theta\, d\theta\, d\phi \qquad (6)$$

Equation (6) describes the contribution to the geoid from the direct gravitational attraction of the surface mass. That surface mass also loads and deforms the underlying solid Earth, which causes an additional geoid contribution:

$$\left\{ \begin{array}{c} \Delta C_{lm} \\ \Delta S_{lm} \end{array} \right\}_{\text{solid E}} = \frac{3k_l}{4\pi a \rho_{\text{ave}}(2l+1)} \int \Delta\sigma(\theta,\phi) \times \tilde{P}_{lm}(\cos\theta) \left\{ \begin{array}{c} \cos(m\phi) \\ \sin(m\phi) \end{array} \right\} \sin\theta\, d\theta\, d\phi \qquad (7)$$

where k_l is the load Love number of degree l [see, e.g., *Farrell*, 1972; *Chao*, 1994, equation (6)]. The total geoid change is the sum of (6) and (7):

$$\left\{ \begin{array}{c} \Delta C_{lm} \\ \Delta S_{lm} \end{array} \right\} = \left\{ \begin{array}{c} \Delta C_{lm} \\ \Delta S_{lm} \end{array} \right\}_{\text{surf mass}} + \left\{ \begin{array}{c} \Delta C_{lm} \\ \Delta S_{lm} \end{array} \right\}_{\text{solid E}} \qquad (8)$$

To summarize these results for ΔC_{lm} and ΔS_{lm} in a more compact form, we expand $\Delta\sigma$ as

$$\Delta\sigma(\theta,\phi) = a\rho_w \sum_{l=0}^{\infty}\sum_{m=0}^{l} \tilde{P}_{lm}(\cos\theta)(\Delta\hat{C}_{lm}\cos(m\phi) + \Delta\hat{S}_{lm}\sin(m\phi)) \qquad (9)$$

where ρ_w is the density of water (assumed throughout this paper to be 1000 kg/m^3), and is included here so that $\Delta\hat{C}_{lm}$ and $\Delta\hat{S}_{lm}$ are dimensionless. Note that $\Delta\sigma/\rho_w$ is the change in surface mass expressed in equivalent water thickness. By noting that the $\tilde{P}_{lm}$ variables are normalized so that

$$\int_0^{\pi} \tilde{P}_{lm}^2(\cos\theta)\sin\theta\, d\theta = 2(2-\delta_{m,0}) \ , \qquad (10)$$

we conclude from (9) that

$$\left\{ \begin{array}{c} \Delta\hat{C}_{lm} \\ \Delta\hat{S}_{lm} \end{array} \right\} = \frac{1}{4\pi a\rho_w} \int_0^{2\pi} d\phi \int_0^{\pi} \sin\theta\, d\theta \times \Delta\sigma(\theta,\phi)\, \tilde{P}_{lm}(\cos\theta) \left\{ \begin{array}{c} \cos(m\phi) \\ \sin(m\phi) \end{array} \right\} \qquad (11)$$

By using (6) and (7) in (8), and using (11), we find a simple relation between ΔC_{lm}, ΔS_{lm} and $\Delta\hat{C}_{lm}$, $\Delta\hat{S}_{lm}$:

$$\left\{ \begin{array}{c} \Delta C_{lm} \\ \Delta S_{lm} \end{array} \right\} = \frac{3\rho_w}{\rho_{\text{ave}}} \frac{1+k_l}{2l+1} \left\{ \begin{array}{c} \Delta\hat{C}_{lm} \\ \Delta\hat{S}_{lm} \end{array} \right\} \ . \qquad (12)$$

Or, conversely,

$$\left\{ \begin{array}{c} \Delta\hat{C}_{lm} \\ \Delta\hat{S}_{lm} \end{array} \right\} = \frac{\rho_{\text{ave}}}{3\rho_w} \frac{2l+1}{1+k_l} \left\{ \begin{array}{c} \Delta C_{lm} \\ \Delta S_{lm} \end{array} \right\} \qquad (13)$$

Using (13) in (9) gives

$$\Delta\sigma(\theta,\phi) = \frac{a\rho_{\text{ave}}}{3} \sum_{l=0}^{\infty}\sum_{m=0}^{l} \tilde{P}_{lm}(\cos\theta)\frac{2l+1}{1+k_l} \times (\Delta C_{lm}\cos(m\phi) + \Delta S_{lm}\sin(m\phi)) \qquad (14)$$

which can be used to find the change in surface mass density from changes ΔC_{lm} and ΔS_{lm} in the geoid coefficients.

Similarly, using (12) in (3) gives

$$\Delta N(\theta,\phi) = \frac{3a\rho_w}{\rho_{\text{ave}}} \sum_{l=0}^{\infty}\sum_{m=0}^{l} \tilde{P}_{lm}(\cos\theta)\frac{1+k_l}{2l+1} \times (\Delta\hat{C}_{lm}\cos(m\phi) + \Delta\hat{S}_{lm}\sin(m\phi)) \qquad (15)$$

which together with (11) gives the change in the geoid from knowledge of the change in surface mass density.

2.1.2. Love numbers. In the calculations below, we use values for k_l computed as described by *Han and Wahr* [1995] using Earth model preliminary reference Earth model (PREM) [*Dziewonski and Anderson*, 1981]. Results for k_l (D. Han, personal communication, 1998) are shown in Table 1 for a few values of l up to 200. Results for other values of $l < 200$ can be obtained by linear interpolation of the Table 1 results. Linearly interpolating the Table 1 results instead of using exact results introduces errors of less than 0.05% for all $l < 200$.

These results for k_l do not include anelastic effects. Those effects increase with increasing period but are apt to be negligible for our applications. For example, *Wahr and Bergen* [1986] concluded that at an annual period the anelastic effects on the $l = 2$ body tide Love number, k_2^{body}, would probably be less than 2%, corresponding to an effect on $(1 + k_2^{\text{body}})$ of less than 1% .

Table 1. Elastic Love Numbers k_l Computed by Dazhong Han as described by *Han and Wahr* [1995], for Earth Model PREM

l	k_l
0	+0.000
1	+0.027
2	-0.303
3	-0.194
4	-0.132
5	-0.104
6	-0.089
7	-0.081
8	-0.076
9	-0.072
10	-0.069
12	-0.064
15	-0.058
20	-0.051
30	-0.040
40	-0.033
50	-0.027
70	-0.020
100	-0.014
150	-0.010
200	-0.007

The $l = 1$ value assumes the origin of the coordinate system is the center of figure of the solid Earth's surface (see text).

Even allowing for larger effects at longer periods, and perhaps a somewhat greater effect for load Love numbers than for body tide Love numbers (since load Love numbers are more sensitive to upper mantle structure where the anelastic effects could be larger), we tentatively conclude that anelasticity would not perturb the results for $(1 + k_l)$ by more than a few percent.

2.1.2. Thin layer assumption. The results above assume a surface mass layer thin enough that $(l + 2)H/a << 1$ for $l \leq l_{\max}$. For the atmosphere, most of the mass lies within 10 km of sea level. As an example, for $H = 10$ km and $l = 60$, $(l+2)H/a \approx 0.1$. This ratio is large enough that the thin layer assumption might not be adequate for atmospheric applications. This problem is presently being investigated, and the results will be reported in a future paper.

2.1.3. Terms with $l = 0, 1$. The terms in (15) with $l = 0$ and $l = 1$ require discussion. The $l = 0$ term is proportional to the total mass of the Earth where "the Earth" includes not only the solid Earth, but also its fluid envelope (the oceans, atmosphere, etc.). This total mass does not change with time, and so ΔC_{00} from GRACE can be assumed to vanish. Suppose, though, the objective is to use (15) to find the geoid contribution from just one component of the surface mass: say, the ocean, for example. The total mass of the ocean need not be constant, due to exchange of water with the atmosphere or the land surface. So the oceanic contributions to $\Delta\hat{C}_{00}$ need not vanish. But this nonzero $\Delta\hat{C}_{00}$ will not induce an $l = 0$ response in the solid Earth: i.e., the load does not cause a change in the total solid Earth mass. Thus $k_0 = 0$.

The $l = 1$ terms are proportional to the position of the Earth's center of mass relative to the center of the coordinate system and so depend on how the coordinate system is chosen. One possibility is to choose a system where the origin always coincides with the Earth's instantaneous center of mass. In that case all $l = 1$ terms in the geoid are zero by definition, and so the GRACE results for $\Delta C_{lm} = \Delta S_{lm} = 0$ for all $l = 1$. Again, the $l = 1$ coefficients for an individual component of the total surface mass need not vanish. Redistribution of mass in the ocean, for example, can change the center of mass of the ocean. But that will induce a change in the center of mass of the solid Earth, so that the center of mass of the ocean + solid Earth remains fixed. So, for this choice of coordinate system, $k_{l=1} = -1$.

Another possibility is to define the coordinate system so that its origin coincides with the center of figure of the Earth's solid outer surface. That is the usual way of defining the origin, since the coordinate system is determined using geodetic measurements of positions on the solid Earth's surface. In that case the $l = 1$ GRACE results for $\Delta C_{lm} = \Delta S_{lm}$ need not vanish, and the Love number $k_{l=1}$ is defined so that the $l = 1$ terms in (15) describe the offset between [the center of mass of the surface mass + deformed solid Earth] and [the center of figure of the deformed solid Earth surface]. It is shown by *Trupin et al.* [1992; equation (10)] that for this coordinate system $k_{l=1} = -(h_{l=1}+2l_{l=1})/3$, where $h_{l=1}$ and $l_{l=1}$ are the $l = 1$ displacement Love numbers when the origin is the center of mass of the deformed solid Earth. For this choice of origin, the numerical value of $k_{l=1} = -(h_{l=1} + 2l_{l=1})/3$ is given in Table 1.

2.2. Data Sources

One of our goals in this paper is to estimate the time-dependent contributions to the geoid caused by mass redistribution in the ocean, in the atmosphere, and in continental water storage. To do this we start with global, gridded mass fields for each of these quantities, integrate over latitude and longitude using (11) to find the $\Delta\hat{C}_{lm}$ and $\Delta\hat{S}_{lm}$; and then use those coefficients in (15) to find the geoid change as a function of position on the Earth's surface.

2.2.1. Ocean Mass. To estimate the redistribution of mass in the ocean, we use output from a variant of the Parallel Ocean Program (POP) model developed at Los Alamos National Laboratory [*Dukowicz and Smith*, 1994]. In this variant model, as modified at the National Center for Atmospheric Research (NCAR), a generalized coordinate system is adopted following a suggestion of *Smith et. al.* [1995], such that the coordinate system north pole is shifted from the geographical

north pole to a point over land. This allows the inclusion of the Arctic Ocean without the problem of grid point singularities associated with the convergence of meridians at the pole. The model is integrated on a global grid with 192 (longitude) x 128 (latitude) x 32 (depth) points yielding an average horizontal resolution of approximately 150 km and vertical resolution varying from 25 m near the sea surface to 300 m in the deep ocean. The ocean in this model includes a free surface, thus allowing the air-sea interface to evolve freely and permitting the use of realistic, unsmoothed (at the grid scale) bathymetry. The model is driven by 6 hourly surface winds generated by the European Centre for Medium-Range Weather Forecasts (ECMWF) for the period 1986 to 1996. Surface fluxes of heat and salt are predicted as being linearly proportional to the difference between climatological monthly mean values of an "effective" atmospheric temperature [*Barnier et al.*, 1995] and observed sea urface salinity [*Levitus et al.*, 1994] and the model predicted sea surface temperature and salinity. Forcing from atmospheric pressure variations is not included in the experiment considered in this analysis. Instead, the ocean's response to pressure will be combined with our estimates of atmospheric mass variability, as described in section 2.2.3.

The model solution for sea surface height, potential temperature, and salinity was sampled every 3 days between January 1, 1987, and January 1, 1996. The potential temperature and salinity results were used in an equation of state [*Bryan and Cox*, 1975] to estimate the change in density $\Delta\rho(z,\theta,\phi)$ within the ocean (z is depth). The change in ocean mass per unit area $\Delta\sigma$ is found by integrating

$$\Delta\sigma(\theta,\phi) = H(\theta,\phi)\rho_0 + \int_{\text{ocean depth}} \Delta\rho(z,\theta,\phi)dz \quad (16)$$

where H is the change in sea surface height and ρ_0 is the ocean's unperturbed density ($10^3\,\text{kg/m}^3$).

The ocean model is formulated using the Boussinesq approximation and consequently conserves oceanic volume and not mass. To correct for this, we follow the suggestions of *Greatbatch* [1994] and *Dukowicz* [1997] an adjust the sea surface height in each sample by adding a global layer of uniform thickness. The thickness of that additional layer is determined by requiring that the total oceanic mass be equal to the total mass at the initial time step. Note that this correction ignores any actual change in total ocean mass or volume due to net exchange of water with the atmosphere or land surface. We find that the thickness of this additional layer varies by less than 6 mm during a year and that its effects on geoid variability are less than 10 percent of the total oceanic effects.

It is beyond the scope of the present study to assess the accuracy of the model predictions. *Fu and Smith* [1996] compared the sea surface variations predicted by the original Los Alamos version of the POP model, with 2 years of sea surface observations from the TOPEX/POSEIDON altimeter. They concluded that the model did a good job of reproducing sea surface variability over a wide range of scales but that it underestimated the overall variance in sea level by about a factor of 2. The discrepancy was largest at spatial and temporal scales representative of mesoscale eddies: spatial scales less than 300 km and timescales shorter than 3 months. Amplitudes and phases for large-scale, seasonal variations appeared to be well represented by the model. *Chao and Fu* [1995] compared the sea level variability simulated by a model with resolution comparable to that used in this study with TOPEX/POSEIDON observations and found that for large spatial scales the model simulation was quite accurate for timescale down to about 20 days. Whether these general conclusions about the error in the model are also appropriate for the variability in the vertically integrated mass is unknown. In fact, assessments of this sort are likely to be among the first applications of GRACE data, once those data become available.

2.2.2. Continental water mass. To estimate the change in water storage on continents, we use a global, gridded [soil moisture] + [snow mass] data set (provided by Jae Schemm and Huug van den Dool), generated at the National Oceanic and Atmospheric Administration Climate Prediction Center using the method described by *Huang et al.* [1996]. Briefly, observed precipitation and temperatures are used to estimate gridded values of [precipitation]-[evapotranspiration]-[runoff]-[percolation into lower layers] = change in [soil moisture]+[snow mass], at monthly intervals. The grid dimensions are 192 (longitude) x 94 (latitude). No attempt is made to estimate variability on the Antarctic continent. Global, monthly results exist for 1979-1993.

The accuracy of these data are even harder to assess than the accuracy of the ocean model results described above. *Huang et al.* [1996] found good agreement between the model predictions and an independent soil moisture data set for Illinois. But, results for regions with sparse precipitation and temperature observations are apt to be more poorly determined. Also, this data set does not attempt to include changes in water storage beneath the soil layer: that is, beneath about 1-2 m depth. Variations in water storage at those greater depths could well have important effects on the geoid but are not included in our estimates.

2.2.3 Atmospheric mass. The atmosphere is very nearly hydrostatic: the change in atmospheric pressure at a point on the Earth's surface is proportional to the change in total atmospheric mass integrated vertically above that point:

$$\Delta P(\theta,\phi) = g \int_{\text{atmosphere}} \Delta\rho(r,\theta,\phi)dr = g\,\Delta\sigma(\theta,\phi) \quad (17)$$

So for the atmosphere,

$$\Delta\sigma(\theta,\phi) = \frac{\Delta P(\theta,\phi)}{g} \quad (18)$$

Thus global, gridded values of the change in pressure ΔP can be used in (18) to find the change in atmospheric mass density. The results for $\Delta\sigma$ found in this manner will include the effects of changes in water vapor mass as well as changes in the dry air mass: that is, it is the total mass of the air column that is close to being in hydrostatic equilibrium.

To estimate the change in atmospheric mass, we use 3 years (1993-1995) of 6-hourly global pressure fields generated by the ECMWF. We do not work directly with these 6-hourly fields, but instead we add them to form monthly averages and use those averages to compute monthly atmospheric contributions to the geoid. The rationale for averaging these data is that in our case the atmospheric pressure contributions are mostly of interest because, as we will show, they are a source of error when inferring the hydrological signal. Since our hydrological data set consists of monthly averages, working directly with the original 6-hourly pressure data would involve a needless expenditure of processing time.

When we use these pressure data in (18) to find the change in atmospheric mass density, we set the change in atmospheric mass to 0 at every oceanic grid point. The reason is that we expect the ocean response to pressure variations to be very nearly an inverted barometer (IB) response at periods in excess of a few days (for a review, see *Wunsch and Stammer*, 1997). That is, an increase in atmospheric pressure of 1 mbar should cause the underlying ocean surface to depress by 1 cm, so that there is no net change in pressure at the seafloor; or, correspondingly, no net change in mass integated vertically through the overlying ocean and atmosphere. Thus setting $\Delta\sigma = 0$ over the oceans is equivalent to including in $\Delta\sigma$ both the redistribution of atmospheric mass and the redistribution of oceanic mass caused by the atmospheric pressure fluctuations. The oceanic response to pressure is not included in the POP model output described in section 2.2.1.

The real ocean does not respond exactly as an IB. Partly, this is because of the ocean's dynamic response to pressure fluctuations, though that tends to be small at the GRACE averaging periods of a couple weeks and longer [see *Ponte*, 1993, Figures 8 and 9]. But even in the infinite period limit, the response differs slightly from IB in order to conserve oceanic mass and because of gravitational forcing from changes in atmospheric mass over continents [see, e.g., *vanDam et al.*, 1997]. These nondynamic departures from IB are relatively small, but nonnegligible. For example, *vanDam et al.* [1997] used National Meteorological Center (NMC) pressure fields to study both of these effects. They concluded that (1) the global constant that must be added to the IB response to conserve mass typically varies by 2-3 cm over the course of a year (comparable to the local static IB response in the tropics) and (2) gravitational forcing can cause a departure from IB near coastlines that can occasionally be as large as 3-4 cm within a few hundred kilometers of shore (though departures of less than 1 cm are more typical). These effects are large enough that they will probably need to be included when analyzing and interpreting real GRACE data. But because they are, in general, small relative to the other signals we are considering here, we have simplified our computations by ignoring them in our simulations.

Global pressure fields generated by forecast centers such as the ECMWF provide an acceptable, though still not perfect, measure of pressure variability over the globe [*Trenberth and Guillemot*, 1994]. The data are particularly good over continents, which, if the IB response is included, is the only place they are needed. We envision that when using time variable gravity data from a mission such as GRACE to learn about hydrological, oceanic, or geophysical processes, forecast pressure fields would be used to first remove the atmospheric contributions over continents. For some applications, it may be desirable to also remove the effects of the nondynamic departure of the ocean from IB, computed from the pressure fields as described above. This issue is discussed in more detail in section 5.

But the forecast pressure fields are not perfect, and any errors in those fields will degrade the hydrological, etc., results. To approximate the effects of those errors on time variable gravity, we will estimate the error δP in the monthly averaged ECMWF pressure fields by taking the difference between the ECMWF monthly averaged fields and the monthly averages of the corresponding fields generated by the National Meteorological Center (NMC) and dividing that difference by $\sqrt{2}$:

$$\delta P(\theta,\phi) = \frac{P_{\mathrm{ECMWF}} - P_{\mathrm{NMC}}}{\sqrt{2}} \tag{19}$$

We divide by $\sqrt{2}$ with the idea that the two data sets (ECMWF and NMC) each contribute half of the variance in $(P_{\mathrm{ECMWF}} - P_{\mathrm{NMC}})$. Over the oceans we assume that $\delta P = 0$, again consistent with the IB assumption.

This approach could conceivably underestimate the size of the pressure errors, since δP would not include errors common to both data sets. On the other hand, the results do not take into account any possible improvements that might occur in modeling atmospheric pressure by the time GRACE is launched in 2001.

2.2.4 Postglacial rebound. The primary focus of this paper is on the hydrological and oceanic contributions to time variable gravity. One of the issues for recovering those contributions with GRACE is understanding how gravity signals from solid Earth processes might leak into the satellite solutions. To consider this issue we require an estimate of those gravity signals.

By far the largest time-varying signal caused by a solid Earth process comes from postglacial rebound (PGR), the continuing rebound of the Earth in response to the melting of the ice at the end of the last ice age. In this paper, we estimate the effects of PGR by convolving load Love numbers for a viscoelastic Earth, computed as described by *Han and Wahr* [1995], with *Tushing-*

ham and Peltier's [1991] Ice-3G Pleistocene ice model. We presume that anyone interested in extracting hydrological or oceanic signals from satellite gravity data would first remove a modeled PGR solution of this type. But any such model would undoubtably contain errors, due to uncertainties both in the ice model and in the Earth's viscosity profile. Those errors are likely to be substantially reduced after GRACE has been in orbit for a number of years, since by then GRACE analyses will presumably have been able to isolate and remove the PGR signal, at least over Canada and Scandinavia [see, e.g., *Dickey et al.*, 1997]. But since in the meantime people will be relying on existing PGR models, it is desirable to obtain some estimate of the model uncertainties.

For the applications discussed in this paper, we assume the ice deglaciation is perfectly known and that the only error in the viscosity model is an incorrect value for the viscosity of the lower mantle (the region of the mantle below 670 km depth). Specifically, we assume the real Earth has an elastic lithosphere of thickness 120 km, a uniform upper mantle viscosity of 10^{21} Pa s, and a uniform lower mantle viscosity of 10^{22} Pa s. But we assume that the model used to estimate the effects, while having those same values of lithospheric thickness and upper mantle viscosity, has a lower mantle viscosity of 5×10^{22} Pa s. We assume that the model uses Ice-3G and that Ice-3G is correct. Thus we estimate the PGR error as the difference between two model runs: one with a lower mantle viscosity of 10^{22} Pa s and the other with a lower mantle viscosity of 5×10^{22} Pa s.

This simple approach underestimates the number of ways in which the model can be in error. The Ice-3G ice model is almost certainly not correct, and in fact, *Peltier* [1994] has recently constructed an improved ice model which he calls Ice-4G. The lithospheric thickness and upper mantle viscosity could well differ from our nominal values. In fact, the assumptions about uniform viscosities throughout the upper and lower mantles is probably a gross oversimplification. The Earth's viscosity and lithospheric thickness could even have significant lateral variability. An attempt to meaningfully address all these possible problems lies well beyond the scope of this work. Instead, we have focused only on the effects of an error in the lower mantle viscosity, because that is probably the single parameter with the largest effect on time-dependent gravity at scales of roughly 500 km and larger. The two values 10^{22} Pa s and 5×10^{22} Pa s are both plausible lower mantle viscosities and lead to time-dependent, long-wavelength gravity solutions which tend to be maximally different from one another. We conclude below that at locations which are closer than about 500 km to the centers of rebound, the uncertainty in PGR caused by not knowing the lower mantle viscosity is already large enough to be a significant problem in inferring secular changes in oceanography or hydrology. We expect that even if we could develop some way of meaningfully including other model errors, this general conclusion would not change.

2.2.5. GRACE errors. The accuracy with which GRACE can map the Earth's gravity field is determined by several sources of error, including system-noise error in the satellite-to-satellite microwave ranging measurements, accelerometer error, error in the ultrastable oscillator, and orbit error. The accuracy depends somewhat on the orbital configuration (on the altitude and spacecraft separation, for example), which has not yet been finalized. Here for $l > 1$ we use preliminary accuracy estimates provided by Brooks Thomas and Mike Watkins at Jet Propulsion Laboratory (JPL), which assume a spacecraft altitude of 450 km, a spacecraft separation of 100 km, and an averaging period of 12 days. For $l = 1$ we use estimates from Srinivas Bettadpur from the University of Texas (these estimates are relative to a coordinate system origin coincident with the center of figure of the solid Earth surface). These accuracy estimates are in the form of degree amplitudes of the expected geoid error. Degree amplitudes are defined in the following paragraphs.

Suppose the geoid is averaged over a 12-day interval, and let the error in the GRACE estimate of this averaged geoid be

$$\delta N(\theta,\phi) = a \sum_{l=0}^{\infty} \sum_{m=0}^{l} \tilde{P}_{lm}(\cos\,\theta)(\delta C_{lm} \cos\,(m\phi) + \delta S_{lm} \sin\,(m\phi)) \quad (20)$$

where δC_{lm} and δS_{lm} are the errors in the GRACE geoid coefficients. Then the spatial variance of the geoid error, taken over the entire globe, is

$$\delta\sigma_{\rm sp}^2 = \frac{1}{4\pi} \int_0^{2\pi} d\phi \int_0^{\pi} \sin\,\theta\, d\theta\, \delta N^2(\theta,\phi) = a^2 \sum_{l=0}^{\infty} \sum_{m=0}^{l} (\delta C_{lm}^2 + \delta S_{lm}^2) \quad (21)$$

The degree amplitude of the GRACE error is defined as

$$\delta N_l = a \sqrt{\sum_{m=0}^{l} (\delta C_{lm}^2 + \delta S_{lm}^2)}\ , \quad (22)$$

so that δN_l^2 is the total contribution to the variance of the GRACE geoid error from all terms of degree l. The degree l is a measure of the spatial scale of a spherical harmonic. The half-wavelength of a (l,m) spherical harmonic serves as an approximate representation of the spatial scale and is roughly $(20{,}000/l)$ km. So δN_l^2 is a measure of the contribution to the variance from all terms of a given spatial scale.

We will assume here that the uncertainties in the GRACE estimates of C_{lm} and S_{lm} depend on l but not on m (i.e., that the geoid error depends on wavelength but not on spatial orientation) and that the errors in

coefficients with different values of l and m are uncorrelated (equivalent to assuming that, on average, GRACE will determine the geoid equally well over all regions of the globe). The geoid uncertainties can then be summarized by providing estimates of the expected δN_l as a function of l, and this is the form in which the uncertainties were provided to us by Thomas and Watkins. Since each δN_l involves the sum over $2l+1$ geoid coefficients (note that $S_{l0}=0$ for each l), then an individual uncertainty δC_{lm} or δS_{lm} is equal to δN_l divided by $\sqrt{2l+1}$.

The uncertainties in the 12-day averages can be used to estimate uncertainties for longer averaging times, assuming the errors are uncorrelated from one averaging period to the next. For example, the uncertainties δN_l for a 30-day average should equal the 12-day uncertainties multiplied by $\sqrt{12/30}$.

We can extend these definitions to consider the variance over both space and time. The error in the geoid $\delta N(\theta,\phi,t)$ and in the geoid coefficients $\delta C_{lm}(t)$ and $\delta S_{lm}(t)$ are functions of time t. The combined spatial and temporal variance of the geoid error over the entire globe and over the time interval from 0 to T is

$$\delta\sigma^2_{\mathrm{sp/t}} = \frac{1}{4\pi T}\int_0^T dt \int \sin\theta\, d\theta\, d\phi\, \delta N^2(\theta,\phi,t) = \sum_l \left(\delta N_l^{\mathrm{sp/t}}\right)^2 \quad , \quad (23)$$

where the space/time degree amplitude is

$$\delta N_l^{\mathrm{sp/t}} = a\left[\frac{1}{T}\sum_m \int_0^T \left(\delta C^2_{lm}(t)+\delta S^2_{lm}(t)\right)\, dt\right]^{1/2} \quad (24)$$

For example, suppose the objective is to use GRACE data to find the annually varying components of the geoid during a single year. This would presumably be done by fitting $\cos(\omega t)$ and $\sin(\omega t)$, where $\omega = 1$ cycle per year, to 1 year of 12-day coefficients, for each C_{lm} and S_{lm}. Let δC_{lmc} and δS_{lmc} be the errors in the $\cos(\omega t)$ coefficients of C_{lm} and S_{lm}, and let δC_{lms} and δS_{lms} be the errors in the $\sin(\omega t)$ coefficients. Then $\delta N_l^{\mathrm{sp/t}}$ of the annually varying component of the geoid during the time period $T = 1$ year reduces to

$$\delta N_l^{\mathrm{sp/t}} = \frac{a}{\sqrt{2}}\left[\sum_{l,m}\left(\delta C^2_{lmc}+\delta S^2_{lmc} + \delta C^2_{lms}+\delta S^2_{lms}\right)\right]^{1/2} \quad \text{.... annual} \quad (25)$$

A covariance error analysis for simultaneously fitting $\cos(\omega t)$ and $\sin(\omega t)$ to the geoid coefficients shows that the 1σ GRACE uncertainty in each of C_{lmc} and C_{lms} is equal to the uncertainty in the 12-day average of C_{lm} multiplied by $\sqrt{2/N}$, where $N = 365/12$ is the number of 12-day data points in the 1 year of data. The result is similar for the S_{lm} coefficients. Thus the space/time degree amplitudes of the GRACE error in the annually varying component are given by

$$\delta N_l^{\mathrm{sp/t}} = a\sqrt{\frac{2}{N}}\left[\sum_{m=0}^{l}\left(\delta C^2_{lm}+\delta S^2_{lm}\right)\right]^{1/2} \quad \text{.. annual} \quad (26)$$

for the GRACE errors in the annually varying geoid.

The solid lines in Figures 1a and 1b show the expected GRACE uncertainties $\delta N_l^{\mathrm{sp/t}}$ in the annually varying term after 1 year of data. Note that beyond about l=13 the errors increase with increasing l: that is, with decreasing spatial scale.

The GRACE geoid accuracy estimates used in this paper include the anticipated effects of all GRACE measurement errors. They do not include the possible effects of aliasing of short-period geophysical signals into the long-period GRACE averages. For example, 6-hourly results (not shown) from the ocean model described in section 2.2.1. suggest there are likely to be significant long-wavelength gravity signals at periods of a few days and shorter caused by atmospherically driven barotropic motion in the ocean. Because GRACE samples the Earth's gravity field along its evolving orbital path, these short-period signals will not entirely average out in the 2 to 4-week GRACE averages. There will be similar effects aliasing from short-period atmospheric disturbances (e.g., synoptic-scale storms) and the diurnal and semidiurnal oceanic tides. Global pressure fields and ocean tide models will be used to try to remove these latter signals before processing, but there will undoubtably be errors in both the pressure fields and in the tidal models. The possible aliasing effects of these, and other, short-period signals are presently under study.

3. Hydrological, Oceanographic, and Atmospheric Contributions to Time-Dependent Gravity

The redistribution of water within the oceans, between the oceans and continents, and over the continental surface, can cause changes in the Earth's gravity field. An objective of GRACE is to use the gravity field solutions obtained from the satellite measurements to invert for this redistribution of water. The procedure for doing this and the likely accuracy with which it can be done will be discussed in the following sections. First, though, we discuss the probable size of the hydrological and oceanographic contributions to time-dependent gravity. Atmospheric contributions will also be described, with the rationale that uncertainties in the atmospheric contributions are likely to be a major error source when using GRACE data to determine changes in continental water storage.

We focus especially on the annually varying component, with the expectation that this should be a domi-

nant component of the time variable gravity field. We also assess the relative importance of the nonannual terms.

3.1. Annually Varying Contributions

We use the oceanographic, hydrological, and atmospheric data sets described above to find time series for each $\Delta\hat{C}_{lm}$ and $\Delta\hat{S}_{lm}$ (using (11)), where the time resolution is determined by the data: monthly values for the hydrological and atmospheric data, and 3-day values for the oceanographic data. We fit an annually varying cosine and sine (with t=0 on January 1) to an integral number of years for each of the three time series: 1989-1993 for the hydrological data, 1991-1995 for the oceanographic data, and 1993-1995 for the atmospheric pressure data. We choose 5 years as the nominal data span, since that is the expected duration of the GRACE mission. We use only 3 years of ECMWF pressure data because that is all we have in hand. Once we solve for the annually varying components in each $\Delta\hat{C}_{lm}$ and $\Delta\hat{S}_{lm}$, we use those components in (15) to find the cosine and sine terms in the geoid. The amplitudes of those terms are shown in Plates 1, 2, and 3, for the hydrological, oceanographic, and atmospheric signals. (We do not include the $l = 0$ component when summing in (15), which is equivalent to removing a global mean from these maps. Our rationale is that we anticipate there will be no net mass change for the total Earth system, so that the change in the total $l = 0$ geoid component from all geophysical sources should

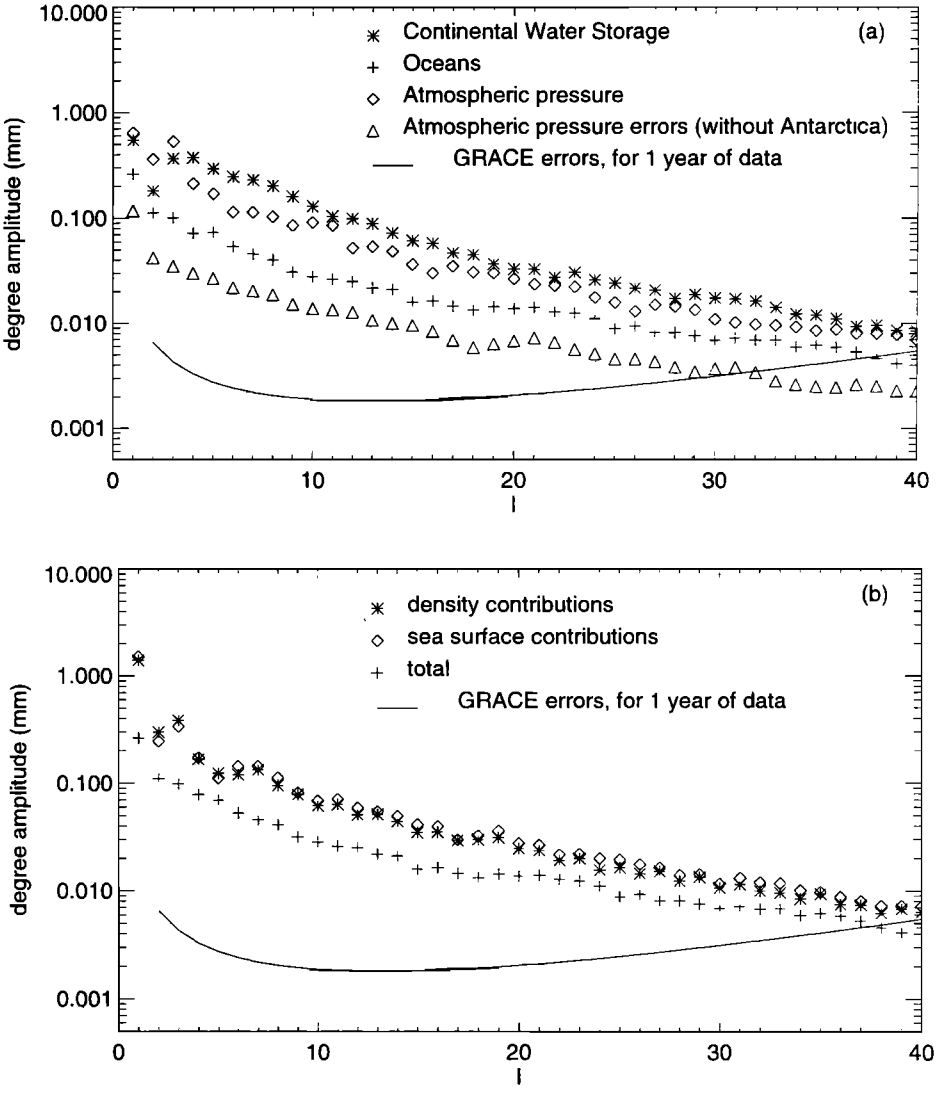

Figure 1. Degree amplitudes for the annually varying component of the geoid. (a) Degree amplitudes for the hydrological, oceanographic, and atmospheric signals as estimated from model output, as well as an estimate of the geoid error introduced by using imperfect atmospheric pressure data to remove the effects of the atmosphere. The errors in the pressure data are estimated as described in the text, and the results shown here do not include the effects of errors over Antarctica. (b) Total annually varying oceanic geoid signal (pluses) separated into contributions from changes in density (asterisks) and from changes in sea level (diamonds). The estimated degree amplitudes of the GRACE errors are shown in both panels as a solid line.

be identically zero.) In addition, Figure 1a shows the space/time degree amplitudes of the annually varying terms (see (25)) for degrees up to l=40 and compares the results with the expected GRACE uncertainties.

The largest single feature in Plates 1-3 is the bullseye over central Asia in the cosine component of the atmospheric contribution (top panel of Plate 3). This feature, which has an amplitude of about 9 mm and is maximum in January, reflects the large annual variation in atmospheric pressure over this region: high pressure in winter, low pressure in summer.

The sine component of the hydrology contribution (bottom panel of Plate 1) includes several features which are almost as large: -6 and -5 mm over southwestern Asia and central Africa, respectively, and 6 and 4 mm over central South America and southern Africa, respectively. Positive values in this panel correspond to a maximum near the March equinox, and negative values correspond to a maximum near the fall equinox. Taken together, the annually varying hydrology contributions tend to be larger than those from the atmosphere. This is evident in Figure 1a, which shows the annually varying hydrology degree variance results are larger than those from the atmosphere for all $l > 3$. Note that the estimates shown in Panel 1 do not include the effects of changes in groundwater storage and so are likely to underestimate the total hydrological contributions.

The annually varying geoid contributions from the ocean are smaller than those from the atmosphere and from hydrology (see Figure 1a), with typical amplitudes of 1.5 mm and less (Plate 2). Note from both panels of Plate 2 that there is a sign difference between the Atlantic Ocean and the Pacific and Indian Oceans. This must be the result of a net transfer of water in the model between the Atlantic Ocean and the Pacific and Indian Oceans at an annual period, with maximum mass in the Atlantic occurring between January and March. This feature appears on Figure 1a as an anomalously large oceanic degree variance at l=1. The size of this feature corresponds to an annual mass variability equivalent to slightly less than 1 cm of sea surface change averaged over the Atlantic Ocean. This corresponds to a relatively small mass transport in and out of the basin: approximately $3 \times 10^4\,\mathrm{m}^3/\mathrm{s}$. This can be compared with the mean flux through Drake Passage into the Atlantic sector of approximately $120 \times 10^6\,\mathrm{m}^3/\mathrm{s}$.

The geoid is insensitive to steric changes in sea level (i.e., effects of changes in density due to variations in temperature or salinity), since those do not involve horizontal transfer of mass. Steric effects can be large, particularly at the annual period where much of the sea surface height variability is caused by thermal expansion and contraction of the water column [see, e.g., *Gill and Niiler*, 1973]. Figure 1b shows the annually varying degree amplitudes (25) for the contributions from the change in water density, from the change in sea surface height, and from the sum. The density and sea surface contributions have about the same amplitudes, and their individual effects are notably larger than the sum of the two contributions. The explanation is that in summer, say, the water column warms and expands, decreasing its density and causing the sea surface to rise. The sea surface contribution to the geoid is thus positive, the contribution from the change in density is negative, and the sum of the two contributions is zero since there is no net change in the mass of the water column. Figure 1b suggests that these steric effects dominate the sea level record at the annual period.

Our estimate of the errors in the annually varying atmospheric pressure contributions to the geoid (not shown here but computed using $(P_{\mathrm{ECMWF}} - P_{\mathrm{NMC}})/\sqrt{2}$ as described above) are large over Antarctica: about 6 mm in the cosine component. This difference reflects a significant bias between the NMC and ECMWF annually varying pressure fields over Antarctica. The Antarctic cosine component of the annually varying pressure has an amplitude of -2 to -3 mbar in the ECMWF fields, and -15 to -20 mbar in the NMC fields. If these estimates are a true representation of the geoid errors computed from, say, the ECMWF pressure fields, they suggest it will be difficult to learn about the annually varying snow/ice signal on the Antarctic continent. In other continental regions the NMC and ECMWF results for the annually varying geoid differ by about 1 mm over Greenland and a few areas in central Asia but otherwise are nowhere larger than a few tenths of a millimeter.

Figure 1a shows the estimated degree amplitudes of the error in the annually varying atmospheric pressure contributions, except that the effects of pressure errors over Antarctica have not been included. Note that the atmospheric errors are 10-20% of the total atmospheric contributions, implying that 80-90% of the annually varying atmospheric signal can be removed from the geoid by using atmospheric pressure fields. The remaining atmospheric signal is 10-20% of the water storage signal, and so might be expected to contaminate water storage estimates at about this level. Note that the degree amplitudes of the atmospheric pressure errors are a much larger fraction of the oceanic degree amplitudes. However, because the IB assumption has been used to generate the atmospheric results, there are no contributions from atmospheric pressure errors over the ocean. Thus the atmospheric errors displayed in Figure 1a do not map directly into errors in the retrieval of oceanic mass. This issue will be discussed in more detail in section 5.

3.2. Nonannual Contributions

Figure 1 and Plates 1-3 represent only the annually varying terms in the geoid. The contributions at other periods are difficult to represent in map form, but their importance can be assessed by considering the signal in the form of degree amplitudes. We compute the geoid contributions at monthly intervals from 5 years of soil moisture data (for 1989-1993) and oceanographic data

(for 1987-1991). We compute a time series of the degree amplitudes for both data sets and then separate the time series into the sum of an annually varying series, a series that contains all variability at periods greater than 1 year (and $\leq$ 5 years), and a series with all variability at periods less than 1 year (and $\geq$ 2 months). Figure 2 shows the rms of those three series, for both the soil moisture data (Figure 2a) and the oceanographic data (Figure 2b). These quantities are equivalent to the space/time degree amplitudes defined in (24).

The soil moisture results are evidently dominated by an annual signal at values of l less than about 20 (corresponding to half-wavelengths of about 1000 km and larger). At larger values of l (i.e., shorter wavelengths), long-period variability begins to dominate. Shorter-period variations tend to remain relatively less important, though it should be remembered that these data are monthly averages and so can not resolve the timescales of individual, broad-scale precipitation events.

For the ocean the short-period variability provides the largest signal at all spatial scales. In fact, when we use the 3-day POP output before constructing these monthly averages, we find (not shown) that the contributions remain large down to 6-day periods, at all spatial scales. These large oceanic effects at short periods are characteristic of barotropic motion, which is much more effective than baroclinic motion at trans-

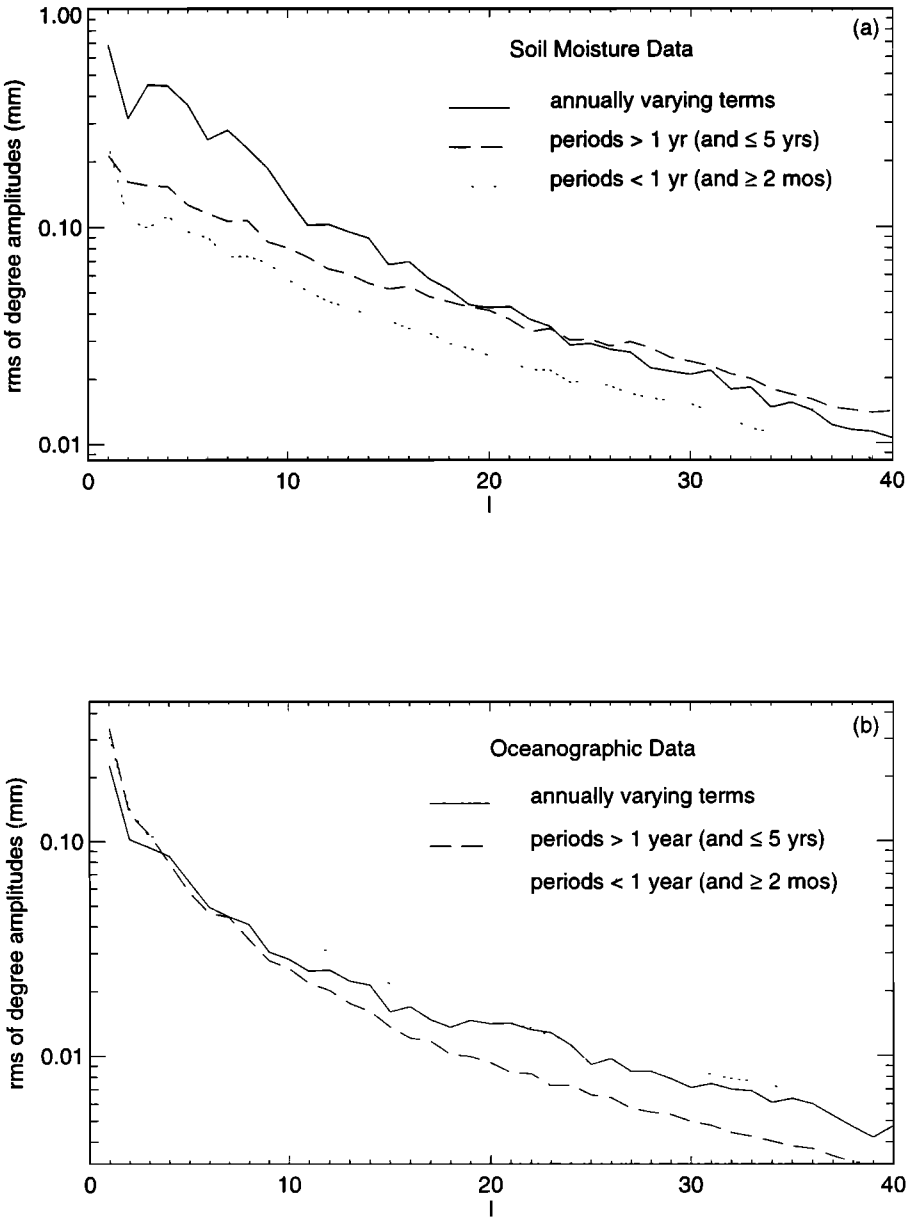

Figure 2. The rms about the mean of 5 years of monthly geoid degree amplitudes, for (a) the soil moisture and (b) the oceanographic data sets. The rms values are shown as a function of degree and are separated into the contributions from the annually varying terms and those at periods $>$ 1 year and $<$ 1 year.

porting mass laterally. And barotropic waves move quickly. Barotropic Rossby waves, for example, can cross an ocean basin in a matter of a few days to a few weeks, depending on wavelength.

4. GRACE Recovery of Surface Mass

The degree variance results in Figure 1a suggest that the annually varying distribution of water both on land and in the oceans should be detectable with GRACE at spherical harmonic degrees of up to about 40, corresponding to half-wavelengths of about 500 km and larger. One method of using the GRACE data for oceanography will be to combine them with altimeter observations to separate the steric and nonsteric sea surface height contributions. In that case, a relevant issue for GRACE is whether it is accurate enough to be sensitive to the separate density and sea surface contributions. Figure 1b shows that it is.

Figure 1a shows that the atmospheric pressure errors are larger than the GRACE errors for l less than about 30. This implies that at half-wavelengths greater than about 650 km the atmospheric pressure errors, rather than the GRACE measurement errors, will likely be the limiting error source for recovering the annually varying changes in continental water storage. Atmospheric pressure errors will be much less of a problem for oceanic applications, because of the nearly IB response of the ocean to atmospheric pressure variations. This will be discussed in more detail in section 5.

But a degree variance comparison is not necessarily the most meaningful way to assess the resolving power of GRACE. We expect that most applications will involve the recovery of signals with known spatial patterns. Any spatial pattern can be represented as a sum of spherical harmonics. Assuming the GRACE errors for the individual coefficients are reasonably uncorrelated, the GRACE measurement error for signal recovery, given as a fraction of the signal amplitude, tends to decrease as $1/\sqrt{M}$, where M is the number of coefficients that make important contributions to the spatial pattern. The implication is that GRACE can likely deliver useful results for signals with known spatial patterns at shorter spatial scales than those suggested by Figures 1a and 1b.

Perhaps the most useful and most general method of inferring changes in surface mass from the GRACE geoid coefficients is to estimate spatial averages. The next three sections describe how those averages might be constructed and the accuracy with which GRACE could deliver them.

4.1. Spatial Averaging

Equation (14) is the starting point for using GRACE estimates of ΔC_{lm} and ΔS_{lm} to recover changes in surface mass density. Because the errors in the GRACE results become large for large l (see Figure 1a), and because terms with large l values can make important contributions to the sum in (14), the use of (14) as written can lead to highly inaccurate results.

GRACE can, however, deliver useful results for spatial averages of the surface mass density:

$$\overline{\Delta\sigma}(\theta,\phi) = \int \sin\,\theta'\,d\theta'\,d\phi'\,\Delta\sigma(\theta',\phi')\,W(\theta,\phi,\theta',\phi') \tag{27}$$

where $W(\theta,\phi,\theta',\phi')$ is an averaging function. It is useful to expand (27) in terms of the spherical harmonic geoid coefficients ΔC_{lm} and ΔS_{lm} recoverable with GRACE. Using (14) in (27) gives, after some manipulation:

$$\overline{\Delta\sigma}(\theta,\phi) = \frac{a\rho_{\text{ave}}}{12\pi}\sum_{l,m}\tilde{P}_{lm}(\cos\,\theta)\sum_{l',m'}\frac{2l'+1}{1+k_{l'}}$$
$$\times\left[\left(\Delta C_{l'm'}W_{lmc}^{l'm'c}+\Delta S_{l'm'}W_{lmc}^{l'm's}\right)\cos\,(m\phi)\right.$$
$$\left.+\left(\Delta C_{l'm'}W_{lms}^{l'm'c}+\Delta S_{l'm'}W_{lms}^{l'm's}\right)\sin\,(m\phi)\right] \tag{28}$$

where

$$\left\{\begin{array}{c} W_{lmc}^{l'm'c} \\ W_{lms}^{l'm'c} \\ W_{lmc}^{l'm's} \\ W_{lms}^{l'm's} \end{array}\right\} = \int \sin\,\theta\,d\theta\,d\phi \int \sin\,\theta'\,d\theta'\,d\phi'$$
$$\times\left\{\begin{array}{c} \cos\,m'\phi'\,\cos\,m\phi \\ \cos\,m'\phi'\,\sin\,m\phi \\ \sin\,m'\phi'\,\cos\,m\phi \\ \sin\,m'\phi'\,\sin\,m\phi \end{array}\right\}$$
$$\times W(\theta,\phi,\theta',\phi')\tilde{P}_{lm}(\cos\,\theta)\tilde{P}_{l'm'}(\cos\,\theta') \tag{29}$$

For averaging over large regions, the $W_{lmc}^{l'm'c}$, etc., are small for large l,m,l',m', so that the contributions to $\overline{\Delta\sigma}$ from the poorly known $\Delta C_{l'm'}$ and $\Delta S_{l'm'}$ at large values of l',m', tend to be small.

If W is defined so that it depends only on the angle α between the points (θ,ϕ) and (θ',ϕ') (i.e., $W(\theta,\phi,\theta',\phi') = W(\alpha)$, where $\cos\,\alpha = \cos\,\theta\cos\,\theta' + \sin\,\theta\sin\,\theta'\cos(\phi-\phi')$), then (28) and (29) reduce to

$$\overline{\Delta\sigma}(\theta,\phi) = \frac{2a\rho_{\text{ave}}\pi}{3}\sum_{l,m}\frac{2l+1}{1+k_l}W_l\tilde{P}_{lm}(\cos\,\theta)$$
$$\times\left[\Delta C_{lm}\cos\,(m\phi)+\Delta S_{lm}\sin\,(m\phi)\right] \tag{30}$$

where

$$W_l = \int_0^\pi W(\alpha)P_l(\cos\,\alpha)\sin\,\alpha d\alpha \tag{31}$$

and where $P_l = \tilde{P}_{lm=0}/\sqrt{2l+1}$ are the Legendre polynomials.

This idea of constructing spatial averages to compensate for poorly known, short-wavelength spherical harmonic coefficients was developed by *Jekeli* [1981] to improve estimates of the Earth's gravity field. Below, we will use Jekeli's Gaussian averaging function [*Jekeli*,

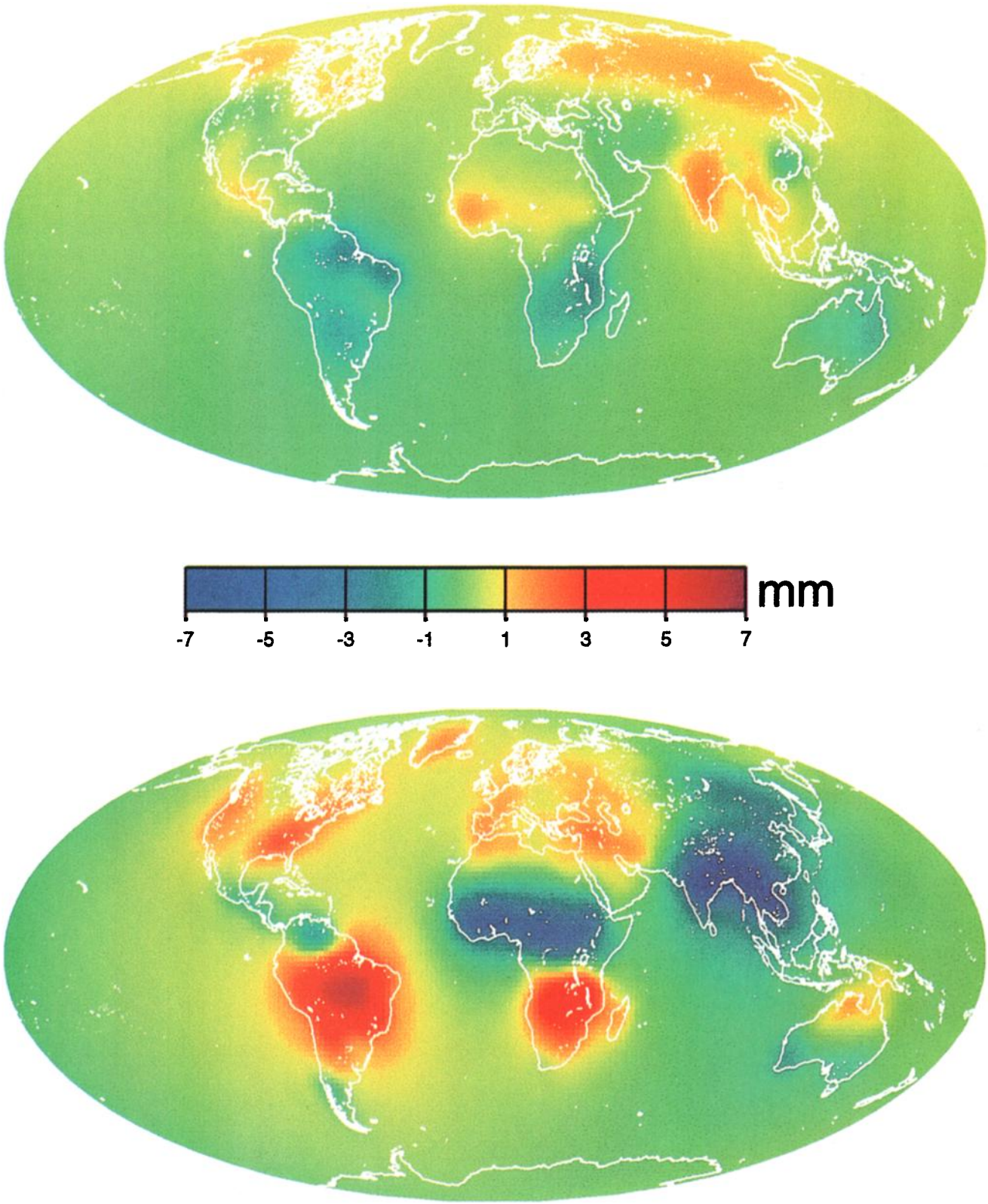

Plate 1. Hydrological contributions to the annually varying geoid component, as estimated from the soil moisture data set described in the text. (top) Cosine component and (bottom) sine component (with t=0 on January 1). These results do not include any effects of groundwater variability.

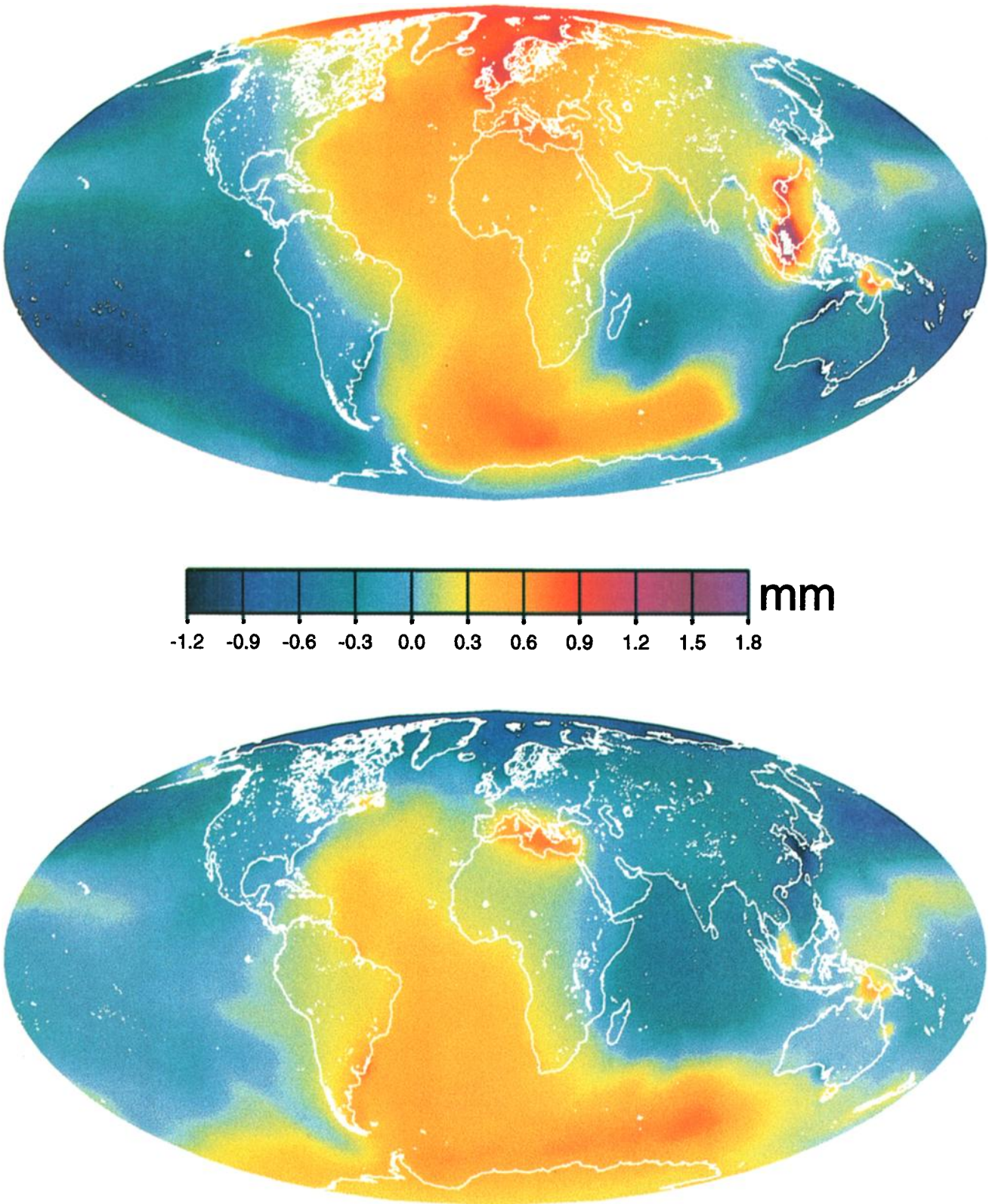

Plate 2. This plate is similar to Plate 1, except it is for the oceanographic contributions to the annually varying geoid.

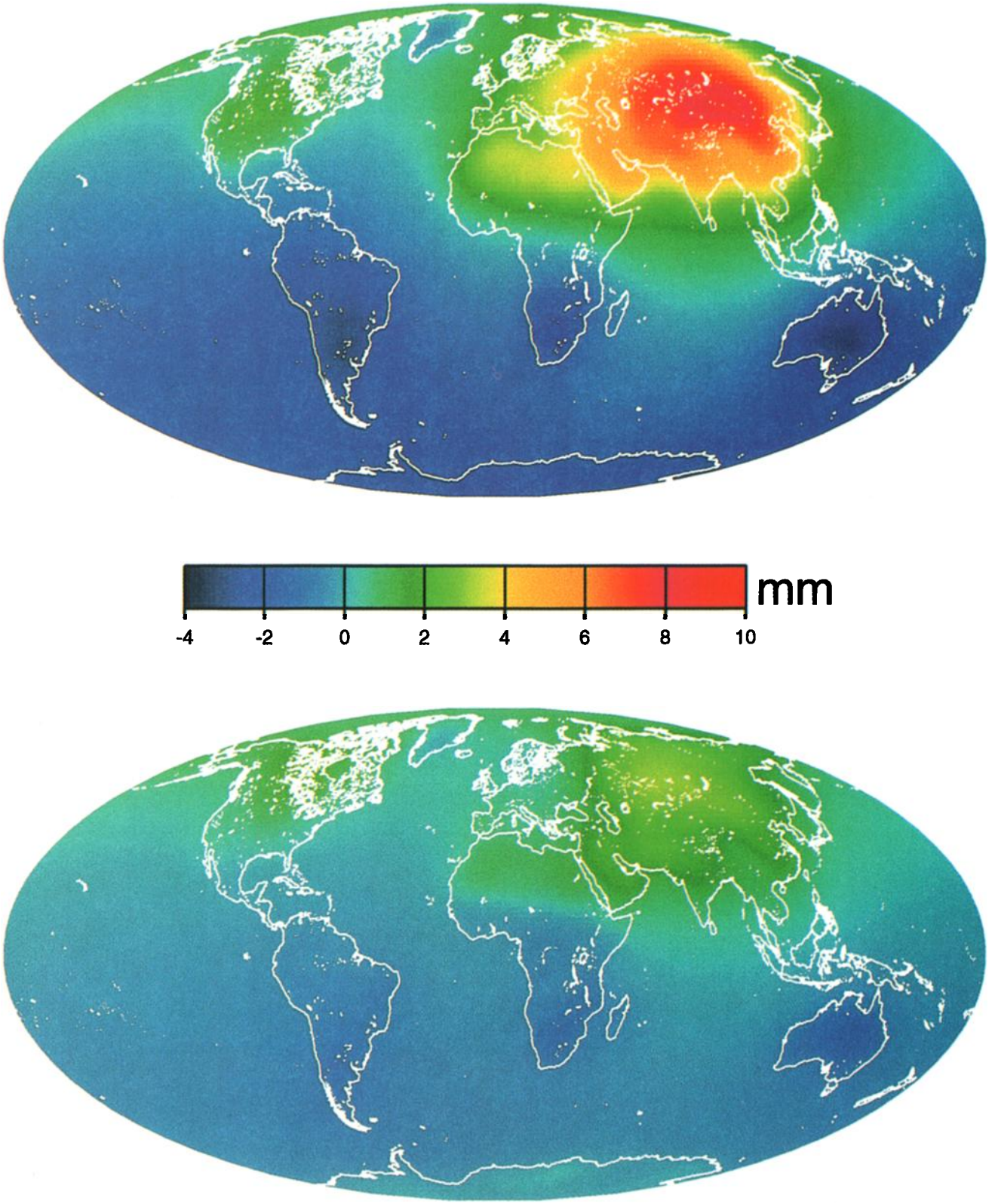

Plate 3. This plate is similar to Plates 1 and 2, except it is for the atmospheric contributions to the annually varying geoid.

1981, eqn. (59)] normalized here so that the global integral of W is 1) where

$$W(\alpha) = \frac{b}{2\pi} \frac{\exp\left[-b(1-\cos\alpha)\right]}{1-e^{-2b}} \tag{32}$$

$$b = \frac{\ln(2)}{(1-\cos(r/a))} \tag{33}$$

and r is the distance on the Earth's surface at which W has dropped to 1/2 its value at $\alpha = 0$ (the distance on the Earth's surface $= a\alpha$). We will refer to r as the averaging radius. *Jekeli* [1981] (normalized version of his equation (63)) shows that the coefficients W_l can be computed with recursion relations:

$$W_0 = \frac{1}{2\pi}$$

$$W_1 = \frac{1}{2\pi}\left[\frac{1+e^{-2b}}{1-e^{-2b}} - \frac{1}{b}\right] \tag{34}$$

$$W_{l+1} = -\frac{2l+1}{b} W_l + W_{l-1}$$

As an example, Figure 3 shows $W(\alpha)$ and W_l for the value $r = 400$ km.

4.2. Reducing Leakage

Suppose the averaging function (32) is used to find the change in seafloor pressure averaged about some oceanic point. Because (32) is nonzero for all values of

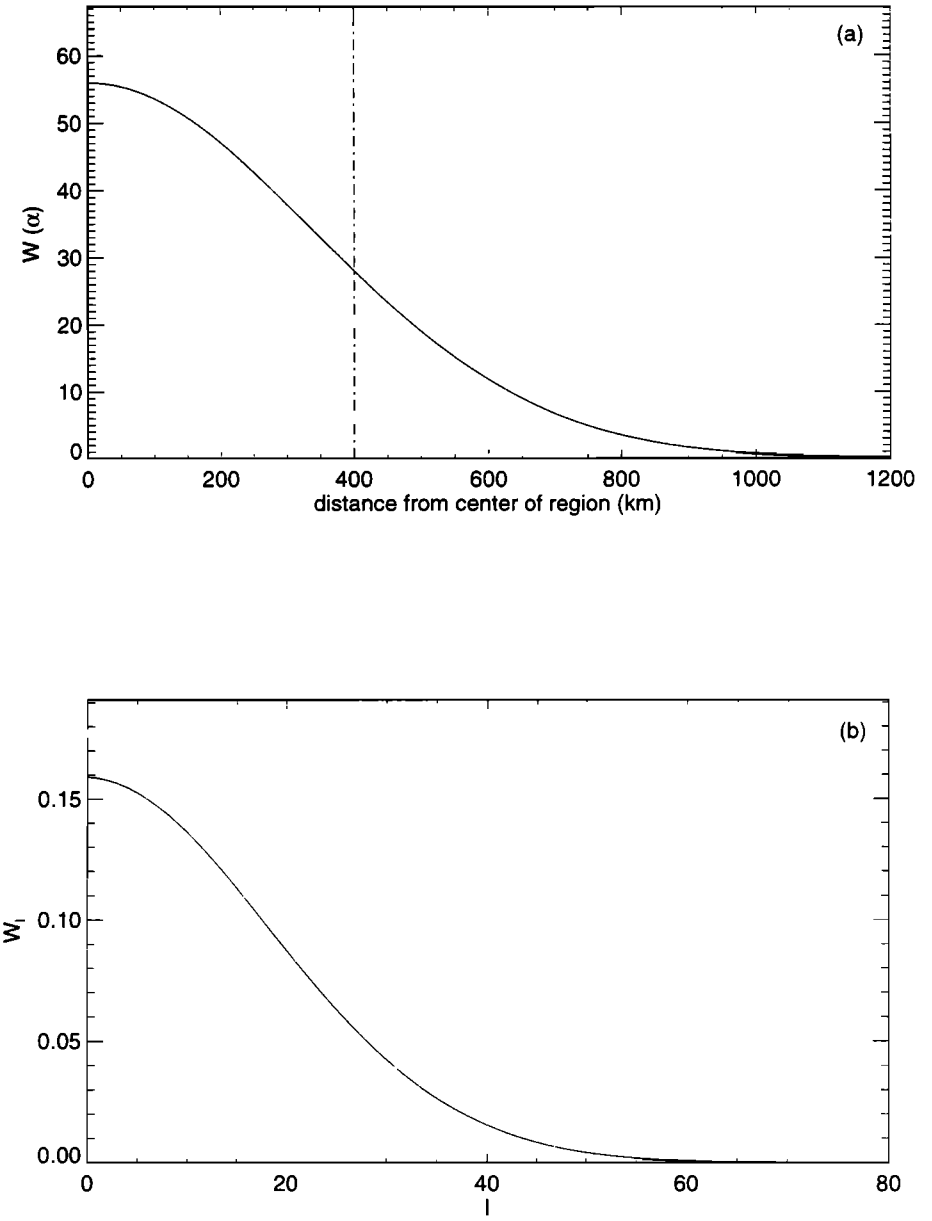

Figure 3. *Jekeli*'s [1981] Gaussian averaging $W(\alpha)$ for an averaging radius of 400 km. (a) W as a function of separation distance ($a\alpha$), where the horizontal line is drawn at 400 km. (b) Spherical harmonic coefficients W_l of this averaging function.

α (see Figure 3), the hydrological and atmospheric pressure signals over continents will leak into the oceanic estimates. Oceanic effects will similarly contaminate hydrological estimates, though the fact that the oceanic signal tends to be smaller than the hydrology signal will probably make this less of a problem.

It may be that this leakage can be reduced by replacing (32) with some other averaging function, designed specifically for the region being considered. The design problems are likely to be somewhat tricky. The seemingly obvious strategy of using an averaging function that entirely vanishes outside the region of interest introduces side lobes into W_l which cause the poorly determined, large-l geoid coefficients to leak into (28). This is discussed in more detail by *Jekeli* [1981].

As an alternative, we have found that when using the averaging function (32) the leakage can be reduced by employing an iterative estimation technique. Suppose, for example, the goal is to estimate seafloor pressure averaged about some oceanic location. Suppose that to obtain accurate GRACE results, the averaging radius must be chosen to be at least as large as some value r. But suppose the location is close enough to shore that the resulting averaging function is large over land, so that the hydrology signal contaminates the seafloor pressure estimate.

This contamination can be reduced by using the GRACE geoid data to first solve for the continental mass distribution, removing the effects of that mass distribution from the GRACE geoid and then using the residual geoid to solve for seafloor pressure. To show how this is done, we choose an averaging radius r_0 for the continental signal. Our studies suggest that in most cases r_0 should be small, though it should be large enough to provide reasonably accurate GRACE averages. For the results described in section 4.3, we will use $r_0 = 250$ km. We use the averaging function described by (32) and (34) (with $r = r_0$ in (33)) in (30) to obtain values of $\overline{\Delta\sigma}$ everywhere over land.

We thus construct a smoothed continental surface mass given by

$$\overline{\Delta\sigma}^{\text{cont}}(\theta,\phi) = C(\theta,\phi)\,\frac{2a\rho_{\text{ave}}\pi}{3}\sum_{l,m}\frac{2l+1}{1+k_l}W_l \times\tilde{P}_{lm}(\cos\,\theta)\,[\Delta C_{lm}\cos\,(m\phi)+\Delta S_{lm}\sin\,(m\phi)] \quad (35)$$

where the land function

$$\begin{aligned} C(\theta,\phi) &= 1 \text{ over land} \\ C(\theta,\phi) &= 0 \text{ over ocean} \end{aligned} \quad (36)$$

has been included in (35) to indicate that $\overline{\Delta\sigma}^{cont}$ is nonzero only over land.

The spherical harmonic coefficients for this smoothed continental surface mass are given by (11) with $\Delta\sigma$ replaced by $\overline{\Delta\sigma}^{\text{cont}}$. Those coefficients can then be used in (12) to estimate the geoid coefficients, $\Delta C_{lm}^{\text{cont}}$, $\Delta S_{lm}^{\text{cont}}$, caused by the continental surface mass. In terms of the original GRACE geoid coefficients, ΔC_{lm} and ΔS_{lm}, and after some algebra:

$$\begin{Bmatrix} \Delta C_{lm}^{\text{cont}} \\ \Delta S_{lm}^{\text{cont}} \end{Bmatrix} = \frac{1}{2}\sum_{l',m'} W_{l'}\frac{(2l'+1)(1+k_l)}{(2l+1)(1+k_{l'})} \times \begin{Bmatrix} F_{lm}^{l'm'}\Delta C_{l'm'} + G_{l'm'}^{lm}\Delta S_{l'm'} \\ G_{lm}^{l'm'}\Delta C_{l'm'} + H_{lm}^{l'm'}\Delta S_{l'm'} \end{Bmatrix} \quad (37)$$

where

$$\begin{Bmatrix} F_{lm}^{l'm'} \\ G_{lm}^{l'm'} \\ H_{lm}^{l'm'} \end{Bmatrix} = \int C(\theta,\phi)\tilde{P}_{lm}(\cos\,\theta)\tilde{P}_{l'm'}(\cos\,\theta) \times \begin{Bmatrix} \cos\,m'\phi\,\cos\,m\phi \\ \cos\,m'\phi\,\sin\,m\phi \\ \sin\,m'\phi\,\sin\,m\phi \end{Bmatrix} \sin\,\theta\,d\theta\,d\phi \quad , \quad (38)$$

and $W_{l'}$ in (37) uses r_0 as the averaging radius.

These estimates of the contributions from continental surface mass can be removed from the original GRACE values to obtain an estimate of the oceanic contributions:

$$\begin{Bmatrix} \Delta C_{lm}^{\text{ocn}} \\ \Delta S_{lm}^{\text{ocn}} \end{Bmatrix} = \begin{Bmatrix} \Delta C_{lm} - \Delta C_{lm}^{\text{cont}} \\ \Delta S_{lm} - \Delta S_{lm}^{\text{cont}} \end{Bmatrix} . \quad (39)$$

When these results for $\Delta C_{lm}^{\text{ocn}}$ and $\Delta S_{lm}^{\text{ocn}}$ are used in (30) to find the averaged surface mass at the original oceanic location, where now the W_l in (30) are computed using the original value r for the averaging radius, the results are relatively free of the effects of surface mass over land. This will be demonstrated in section 4.3.2. A similar approach can be used to remove the contaminating effects of the ocean from estimates of continental water storage.

4.3. GRACE Recovery

We use the results of the preceding two sections, together with simulated GRACE data, to estimate the possible accuracy with which GRACE will be able to recover the oceanographic and hydrological signals. We construct synthetic, monthly geoid coefficients that contain contributions from the redistribution of water on land and in the ocean, errors in the atmospheric pressure contributions, errors in the PGR signal, and simulated GRACE geoid errors. These contributions are modeled as described in section 2.2.

The GRACE geoid errors are estimated using a Gaussian random number generator, where the variance of the Gaussian is defined by the degree amplitude uncertainties described in section 2.2.5. Thus when estimating the GRACE geoid errors, we are ignoring the possibility of correlated errors between geoid coefficients with different l and m variables. The characteristics of the correlated errors depend on the orbital configuration and are likely to be variable during the mission lifetime. These correlations are presently under study, but our preliminary simulations (not shown) that include the correlation estimates suggest that for most

configurations the assumption of perfectly uncorrelated coefficient errors will not affect our general conclusions about GRACE capabilities.

We use our synthetic geoid coefficients in (30) (using (34) to find the averaging coefficients) to estimate the spatially averaged hydrological or oceanographic signals at monthly intervals at various locations on the globe. We include all terms in (30) up to degree and order (i.e., l and m) 150. By comparing with the "correct" hydrological or oceanographic signals, as estimated directly from either the hydrology or oceanography model output that went into the simulation, we are able to assess the accuracy of the GRACE estimates. We emphasize that because we have constructed our synthetic geoid coefficients by including estimated contributions from all the various geophysical sources described above, our hydrology (and oceanography) accuracy estimates include not only the effects of GRACE measurement errors but also the contamination from all the other geophysical signals.

4.3.1 Hydrology. Figures 4a and 4b show 5 years of monthly water storage results Gaussian averaged around Manaus, Brazil (in the Amazon River Basin), in terms of the thickness of a layer of water. The solid line shows the "correct" values as estimated directly from the soil moisture data. The dashed line shows the results estimated from the simulated GRACE geoid coefficients. The two panels show results at two averaging radii: 500 and 230 km. Each panel lists the rms of the monthly values for the "correct" data and for the difference between the "correct" results and the estimates from the simulated GRACE data.

The accuracy of the GRACE results is shown as 0.20 cm for a 500-km averaging radius but has grown to 2.59 cm for a 230-km radius. Even in the 230-km case, the GRACE error is significantly smaller than the "correct" signal, as can be inferred not only from the rms values but just by visually comparing the two time series. (Note, incidentally, that the "correct" results at this location are significantly larger for the 230 km averaging radius than for the 500 km radius. This is because there is more variability in soil moisture in the region immediately adjacent to Manaus than in regions further away.)

Figure 4c shows the rms results for 5 years of monthly averages at Manaus, as a function of averaging radius. The solid line is the rms of the "correct" signal. The dashed line is the rms of the difference between the "correct" signal and the estimates from the simulated GRACE data. The horizontal dash-dot line is 1 cm of water and is included, along with vertical lines at 200, 300, 400, and 500 km, simply as a visual aid. Note that the errors in the GRACE recovery are smaller than the signal at averaging radii of about 190 km and larger and are smaller than 1 cm at radii in excess of about 280 km.

The dotted line shows the rms of the difference between the "correct" results and the GRACE estimates, but now using simulated GRACE data that include only the soil moisture data and the expected GRACE geoid errors. Note, by comparing the dashed and dotted lines, that the GRACE geoid errors dominate at averaging radii below about 250 km. Improvements in the GRACE geoid measurements, particularly at wavelengths of a few hundred kilometers and shorter, could provide better results at those shorter wavelengths.

But as the averaging radius increases further, the contribution from the GRACE geoid errors steadily decreases while the error in the full GRACE recovery remains reasonably constant at about 0.2 cm. At these larger radii it is the error in the atmospheric pressure data that is the limiting source of error for our simulated GRACE results. Thus, assuming our representation of the atmospheric pressure errors is reasonable, we conclude that a reduction in the GRACE geoid errors would be unlikely to significantly improve the GRACE recovery at these larger radii. Instead, the best way to improve the results would be to improve the atmospheric pressure data. This is particularly true for areas such as Antarctica where the atmospheric pressure data are likely to be even more uncertain.

Note the slight increase in the full GRACE recovery errors as the averaging radii increases beyond about 2000 km. This is due to leakage of the ocean signal into the continental estimates at these large radii. This effect can be reduced using the averaging scheme described above.

Figure 5 is similar to Figure 4, expect that it shows results for Rock Island, Illinois (in the Mississippi River Basin). Note that the "correct" signal at Rock Island, as predicted from the soil moisture data set, is smaller, in general, than the signal at Manaus. Still, though, the simulations show that the GRACE errors are smaller than the signal for averaging radii in excess of about 200 km.

The rms of the GRACE errors in this simulation is larger at Rock Island than at Manaus for averaging radii in excess of a few hundred kilometers. This is caused by our simulated errors in the PGR signal. Rock Island is closer to a rebound center (to Hudson Bay, in this case) than is Manaus, so our estimated PGR error has more of an effect. This effect is evident in Figures 5a and 5b as a secular trend in the difference between the GRACE recovery and the "correct" values: the GRACE results tend to be smaller than the "correct" results at the start of the time period, and greater than the "correct" results at the end of the time period. The contamination gets worse at larger averaging radii (Figure 5c) since then the Hudson Bay area gets weighted more heavily into the average. This contamination will be worse at locations closer to the rebound centers (e.g., Hudson Bay, the Baltic Sea, Greenland, and Antarctica).

Our choice of PGR errors (see above) is arbitrary and unlikely to be realistic. We have no way of knowing whether the effects of the PGR errors are either underestimated or overestimated in this simulation. But the

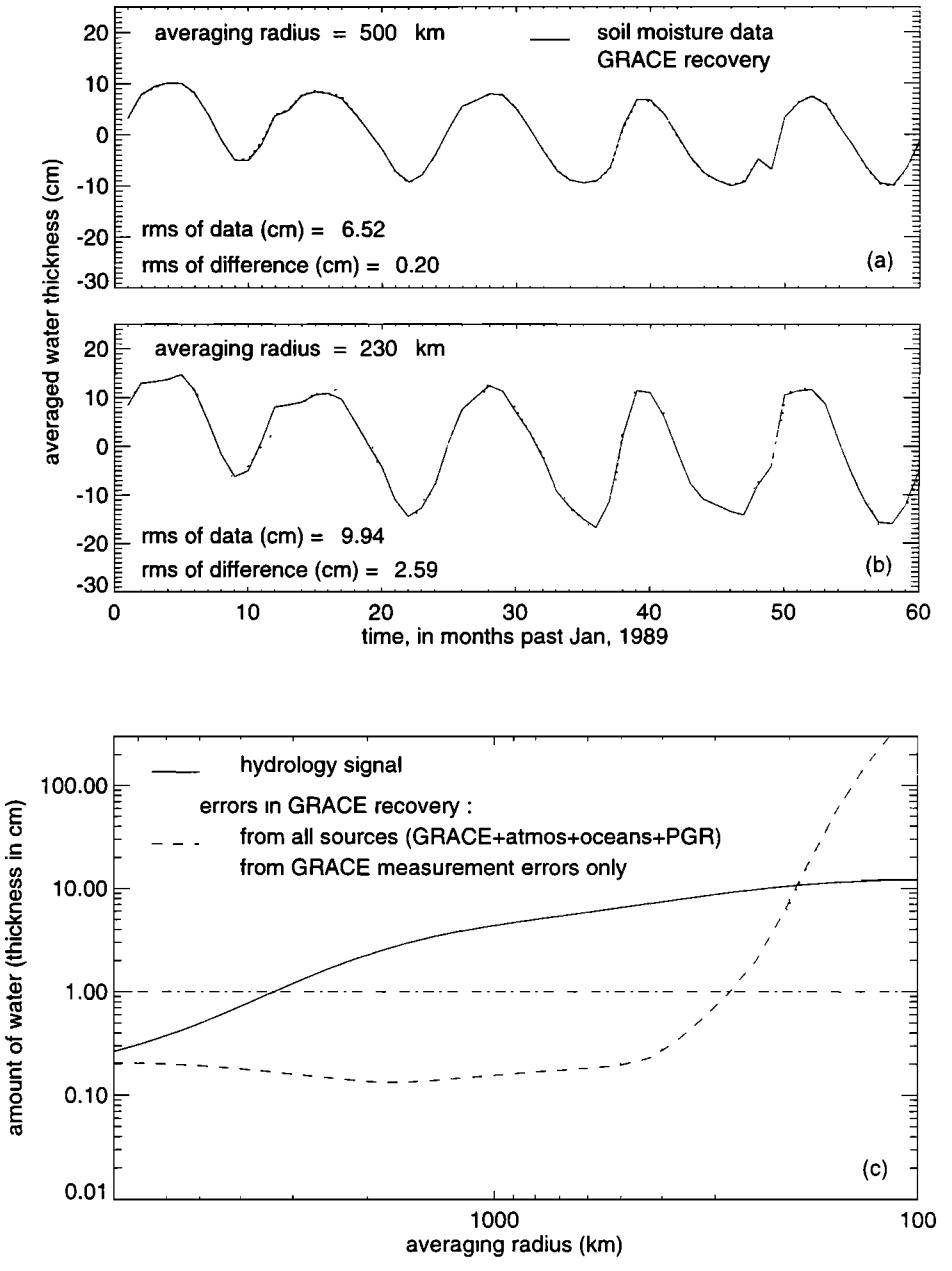

Figure 4. Results of simulations in which synthetic GRACE data are used to recover the hydrological signal at Manaus, Brazil (in the Amazon River Basin). The simulated geoid data include the GRACE geoid errors, as well as contributions from hydrology and oceanography, and our estimated errors in the atmospheric pressure data and in the PGR model. (a,b) Five years of monthly values for two averaging radii. The solid line is the hydrology signal that went into the simulation, and the dotted line is the signal inferred from the synthetic GRACE data. (c) The rms of 5 years of monthly data as a function of averaging radius. The solid line is the estimate from the hydrology data. The dashed line represents the accuracy of the GRACE results, estimated as the rms of the difference between the GRACE recovered values and the hydrology signal. The dotted line is the estimated GRACE accuracy if the only errors were the GRACE geoid errors.

results suggest that caution should be exercised when interpreting secular changes in continental water storage at locations even moderately near a rebound center. At those locations, and depending on the radius and accuracy desired, it may not be wise to put much faith in any derived secular trend in the recovered water storage.

On the other hand, it is likely that after several years of observations, GRACE will have provided enough information about the secular geoid change to permit a substantial improvement in the PGR model. If GRACE water storage estimates are recomputed after removing the improved PGR model, it should be possible to obtain better estimates of the secular water storage trends

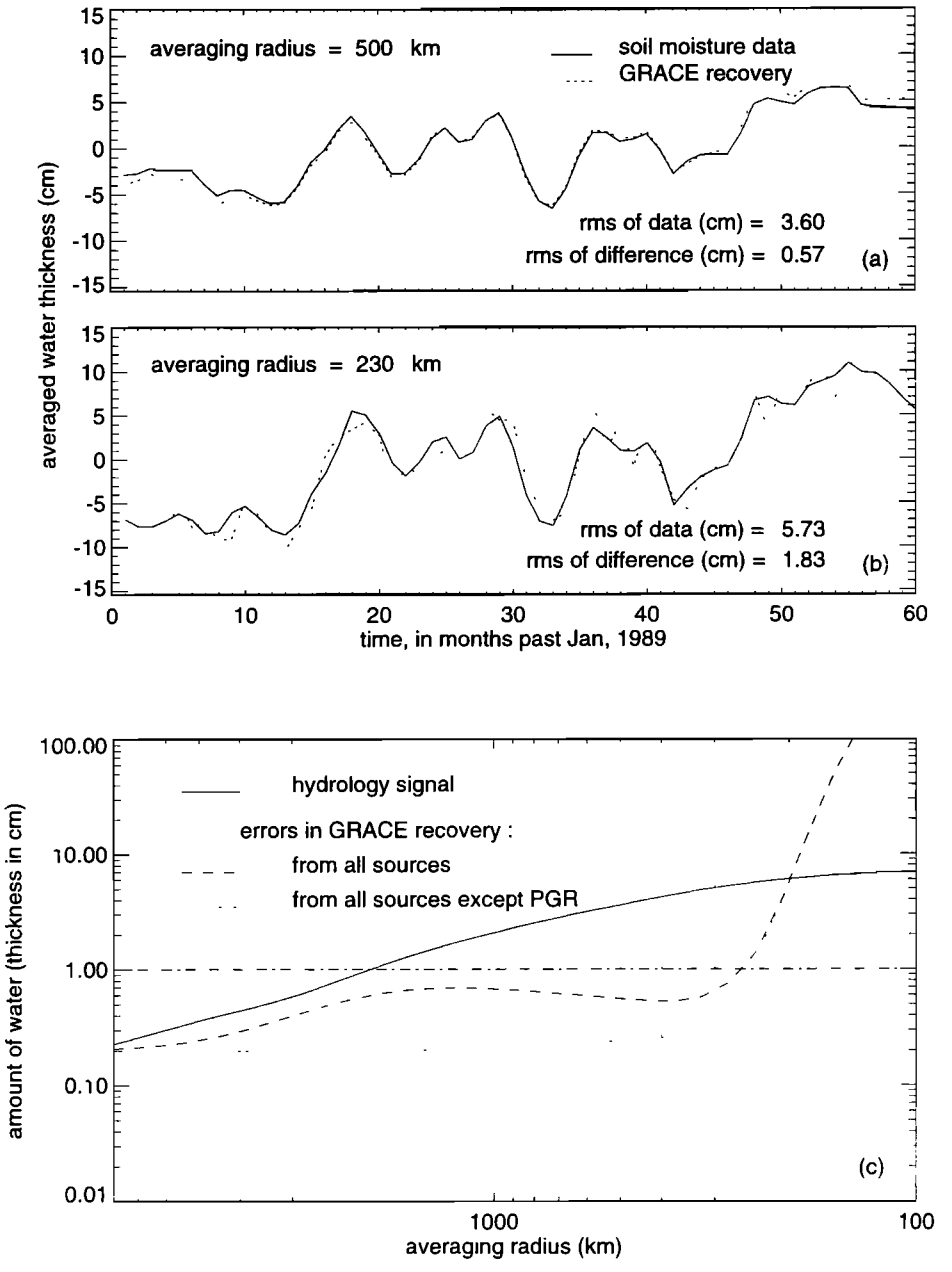

Figure 5. This figure is similar to Figure 4, except for the hydrology signal at Rock Island, Illinois (in the Mississippi River Basin). The dotted line in Figure 5c is computed by not including our estimated PGR errors in the simulation and illustrates the accuracy with which GRACE could determine the nonsecular variability at this location.

for most applications. There are still apt to be problems very close to the rebound centers however, since any secular water storage signal at those locations is likely to be partially absorbed into the PGR model, and so would be removed, erroneously, from the GRACE data before solving for water storage.

The dotted line in Figure 5c shows the simulated GRACE recovery at Rock Island in the absence of a PGR error. The results are much improved and can be interpreted as illustrating either: (1) the accuracy with which GRACE can deliver nonsecular changes in water storage at Rock Island even with large PGR errors; or (2) the accuracy of the GRACE results, including secular terms, if the PGR model can be improved to where it does not notably contaminate the results at Rock Island.

4.3.2. Oceanography. Figure 6, which is similar to Figures 4 and 5, is an example of how well GRACE should be able to recover changes in seafloor pressure at a location in the middle of the North Pacific Ocean (at 180°E, 30°N). Note from Figures 6a and 6b that most of the power in the seafloor pressure data at this location appears to be at subannual periods, which is consistent with the results described in section 3.2. In fact,

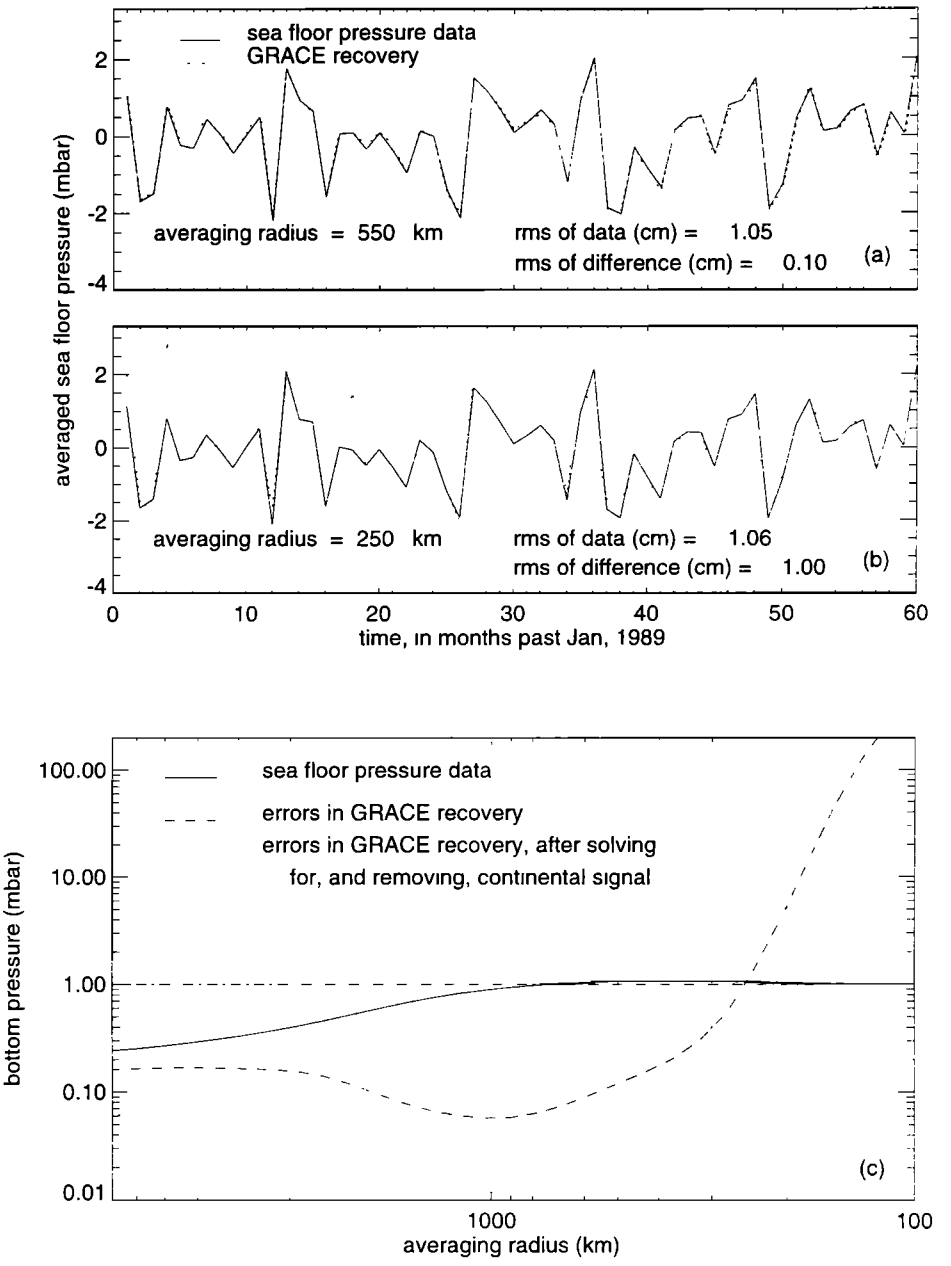

Figure 6. This figure is similar to Figures 4 and 5, except it is for an attempt to recover seafloor pressure at a location in the middle of the North Pacific Ocean (180°E, 30°N). The dotted line in Figure 6c shows the accuracy in the GRACE recovery after solving for, and removing, the continental contributions, as described in the text.

it is difficult to even identify an annually varying signal in these seafloor pressure data. The seafloor pressure amplitudes are, in general, smaller than the soil moisture amplitudes shown in Figures 4 and 5 (1 mbar of seafloor pressure is equivalent to 1 cm of water thickness). As a result, recovery of the oceanographic signal tends to require larger averaging radii than does recovery of the hydrology signal. At the location for Figure 6, the GRACE errors are smaller than the seafloor pressure signal at averaging radii in excess of about 250 km.

Figure 6c shows that the errors in the GRACE recovery are of the order of only 0.05 mbar (equivalent to 0.05 cm of water) at radii close to 1000 km. These errors are substantially smaller than the errors in the hydrology recovery shown in Figures 4 and 5. The reason is that we have assumed that atmospheric pressure data over the ocean will not be removed from the GRACE geoid data, for the reasons described below in section 5. Thus errors in atmospheric pressure data over the ocean have no effect on GRACE surface mass estimates, and so a reduction in the GRACE geoid errors would map directly into an improvement in seafloor pressure recovery at these spatial scales. In contrast, atmospheric pressure errors over land are the principal error source for

GRACE hydrology estimates at averaging radii of several hundred kilometers and larger (see section 4.3.1).

Figure 6c also shows that GRACE recovery errors increase dramatically as the averaging radius becomes larger than about 2000 km. This is caused by leakage of the continental signal into the oceanic estimates. The dotted line shows the improvement in these estimates when the continental signal is removed from the data using the procedure described in (37)-(39).

5. Discussion and Conclusions

The principal conclusion of this paper is that the GRACE satellite, scheduled for a 2001 launch, should be able to recover changes in continental water storage and in seafloor pressure, at scales of a few hundred kilometers and larger and at timescales of a couple weeks and longer. GRACE has the potential of delivering monthly values of surface mass with accuracies approaching 2 mm in water thickness over land, and 0.1 mbar or better in seafloor pressure. These conclusions are based on our analysis of synthetic geoid data and include the effects of contamination from other geophysical signals, as will as the effects of the current best estimates of the GRACE measurement errors.

The scientific potential of these results is described in depth by *Dickey et al.* [1997]. The possible applications are varied and numerous and are summarized briefly here.

The GRACE continental water storage estimates, for example, can be used both for monitoring purposes and to improve understanding of hydrological and atmospheric processes. Because GRACE measurements will consist of averages over hundreds of kilometers, they will complement traditional ground-based hydrological measurements which tend to be restricted to the scales of individual catchments, which are of the order of 10 km or less [see, e.g., *Coughlan and Avissar*, 1996]. The GRACE results can also complement space-based microwave and infrared soil moisture measurements, in that the latter provide information on only the upper few centimeters of water in the soil, whereas the GRACE estimates reflect changes in water storage throughout the water column. The weakness of the GRACE water storage measurements is that they are incapable of distinguishing between water on the surface, in the soil, or in subsoil layers. Neither can GRACE discriminate between water, snow, or ice. The inference of any one of those individual components would require supplementary data or models. What GRACE does allow is closure of the total water budget over large regions. This should permit the assessment and improvement of the hydrological components of climate models and of regional-scale hydrological models. And it could prove useful for helping to monitor the water available for agricultural purposes and to help in assessing flood danger over large regions.

The GRACE oceanographic estimates could be used in several ways. For example, they could be used to help separate the steric from the nonsteric contributions to altimeter measurements of sea surface height. Knowledge of the steric contributions would make it feasible to estimate the change in heat storage over scales of a few hundred kilometers and larger everywhere over the ocean. The gradient of seafloor pressure inferred from the GRACE results could be used, together with the assumption of geostrophy, to infer currents near the seafloor. And, by assimilating both GRACE seafloor pressure results and altimeter sea surface data into ocean general circulation models (OGCMs), it should be possible to largely resolve the ambiguity between barotropic and baroclinic effects that now exists in those models when altimeter data are assimilated alone [e.g., *Cooper and Haines*, 1996].

We have tried to characterize the likely geoid signal, particularly at the annual period, caused by changes in continental water storage, and in the distribution of mass in the oceans and atmosphere. The results are only as good as the hydrological, oceanographic, and atmospheric models they are based on, and the hydrological and oceanographic models are especially difficult to assess. The hydrological results are particularly uncertain, not only because of the extreme difficulty of constructing such a model and of validating the results but also because the hydrology data reflect changes only in soil moisture and snow mass and have no contributions from changes in groundwater.

Our general conclusions about geoid variability, using these data, are that the hydrology contributions are dominated by an annually varying signal that can be as large as half a centimeter in amplitude at certain locations. The oceanographic contributions tend to be smaller than those from hydrology (the annually varying amplitudes are of the order of 1.5 mm or less) and include substantial variability at subannual periods. The annually varying atmospheric contributions are of the same order as the hydrological effects, with the largest atmospheric signal coming from the annual variation of mass over central Asia.

We have described methods for using changes in the GRACE geoid coefficients, ΔC_{lm} and ΔS_{lm}, to estimate changes in surface mass. GRACE will be able to provide useful results only for surface mass averaged over scales of a few hundred kilometers and larger. Equations (28)-(29) describe the most general method of constructing spatial averages of surface mass from the GRACE geoid coefficients, where $W(\theta, \phi, \theta', \phi')$ is an arbitrary averaging function. These equations reduce to (30)-(34) when *Jekeli*'s [1981] Gaussian averaging function (32) is used.

Finally, equations (37)-(39) describe a method for reducing the leakage of continental mass into the GRACE estimates of changes in seafloor pressure. A similar ap-

proach can be used to reduce the leakage of the oceanic signal into the hydrological estimates.

5.1. IB Assumption

When including atmospheric pressure errors in the simulations described above, we ignored the errors over the ocean. This is because for most applications we expect the user will either (1) correct for atmospheric effects by assuming an equilibrium oceanic response to pressure or (2) will not remove either the effects of atmospheric pressure over the ocean or the ocean's response to pressure. Since an equilibrium ocean response is very close to an IB response (see section 2.2.3), and since option 2 is identical to including the effects of pressure + the effects of an IB oceanic response to pressure, then the consequences of options 1 and 2 are almost identical. In either case, atmospheric pressure errors over the ocean would have almost no effect on the results.

To explain our reasoning for how atmospheric pressure is likely to be included in GRACE analyses, we consider several types of applications. Suppose, for example, the objective is to use the GRACE geoid results to estimate either the change in continental water storage, or the redistribution of mass in the solid Earth, or any other process outside of the ocean and atmosphere. In those cases it is desirable to remove from the data the best possible estimate of the geoid contributions caused by the atmosphere and ocean. The complete removal of those contributions would require knowledge of changes in atmospheric pressure, of the redistribution of ocean mass caused by those changes in pressure, and of the response of the ocean to all other meteorological, radiative, and tidal forcing. The effects of ocean tides can and should be removed using the new generation ocean tide models derived from TOPEX/POSEIDON altimeter data (for an intercomparison of recent models, see *Andersen et al.* [1995]. The response of a fully baroclinic ocean to thermal and wind forcing and to the flux of fresh water through evaporation, precipitation, and runoff can probably not be modeled well enough yet to warrant its removal from the GRACE data. By including the POP model output in the simulations described above, we allowed for the leakage of that entire oceanic signal into the hydrology estimates. In contrast, the ocean's response to pressure at the 2-3 week (and longer) averaging times of GRACE is relatively well understood and is close to equilibrium (see section 2.2.3).

So for nonoceanic applications of GRACE, it is desirable to remove the effects of atmospheric pressure using the IB assumption (i.e., no atmospheric pressure variation over the ocean), probably modified by adding a spatially uniform correction to conserve mass, and possibly including the effects of atmospheric gravitational forcing of the ocean (see section 2.2.3). In the exact IB case there are no contributions from atmospheric pressure over the ocean, and so no contamination from errors in the forecast pressure fields in oceanic regions.

Suppose, instead, the objective is to use the GRACE geoid estimates to learn about the ocean. We write the variation in seafloor pressure Δp_b as

$$\Delta p_b = \Delta p_a + \rho_0 g \Delta\eta + \int_{\text{ocean depth}} \Delta\rho(z) g dz \qquad (40)$$

where Δp_a is the variation in atmospheric pressure at the ocean's surface, $\Delta\eta$ is the increase in sea surface height, $\Delta\rho(z)$ is the increase in ocean density at depth z, and ρ_0 is the average water density near the ocean's surface.

We consider three possible oceanic applications of GRACE data.

1. Horizontal derivatives of the GRACE seafloor pressure results are used to infer deep ocean currents.
2. GRACE seafloor pressure measurements and altimeter sea surface height observations are assimilated into an OGCM.
3. Altimeter sea surface height data and GRACE seafloor pressure results are combined to separate steric and nonsteric sea surface height contributions.

Consider, first, applications of type 1. In the geostrophic limit, deep ocean currents are proportional to the gradient of the total bottom pressure, as produced by the total weight of the overlying oceanic and atmospheric mass. Thus for these applications the total bottom pressure as given by (40) is desired, and so the GRACE data should not be corrected for atmospheric pressure over the ocean or for the ocean's response to pressure. The effects of atmospheric pressure over land should still be removed from the GRACE geoid, however, to keep those effects from leaking into the oceanic solutions.

Next, consider applications of type 2. Most OGCMs are run with the goal of understanding the response of the ocean to winds and surface fluxes and do not include forcing from atmospheric pressure fluctuations. Suppose we separate the true sea surface height variability into a component $\Delta\eta_{\text{press}}$ driven by variations in atmospheric pressure, and a component $\Delta\eta_{\text{winds}}$ driven by all other forcing (e.g., by winds, and by surface fluxes of heat and mass). We expect that at the GRACE averaging periods $\Delta\eta_{\text{press}}$ should be well represented by an equilibrium response, so that $\Delta\rho_{\text{press}}(z) \approx 0$ (i.e., an equilibrium response involves no change in density). In that case, (40) can be written as

$$\Delta p_b = (\Delta p_a + \rho_0 g \Delta\eta_{\text{press}}) + \rho_0 g \Delta\eta_{\text{winds}} + \int_{\text{ocean depth}} \Delta\rho_{\text{winds}}(z) g dz \qquad (41)$$

If the OGCM does not include pressure forcing, then $(\Delta p_a + \rho_0 g \Delta\eta_{\text{press}})$ should be removed from the GRACE estimates of Δp_b before assimilation. This is equivalent to removing the effects of atmospheric pressure and of the ocean's response to atmospheric pressure from

the GRACE data. Note that $(\Delta p_a + \rho_0 g \Delta\eta_{\text{press}})$ is small and vanishes identically if the equilibrium solution $(\Delta\eta_{\text{press}})$ can be approximated by an IB response.

Finally, consider applications of type 3. The altimeter sea surface height data reflect the sum of steric (i.e., caused by changes in density) and nonsteric (caused by changes in mass) effects. The GRACE seafloor pressure measurements are sensitive to changes in mass and so can be used to help determine the nonsteric sea surface height component. But this requires that the effects of redistribution of mass in the atmosphere (i.e., atmospheric pressure) over the ocean be removed from the GRACE data, without removing the ocean's response to pressure: P_a should be removed from P_b in (40). So, this is one case where it would be logical to remove atmospheric pressure over the oceans from the GRACE data, with the consequence that errors in the atmospheric pressure fields would contaminate the results.

On the other hand, it is the comparison between altimeter and seafloor pressure measurements that is important for these applications, and the ocean's equilibrium response to pressure is nonsteric and so shows up in both data sets. As a result, these studies would reach the same conclusions about the steric sea surface height contributions if the GRACE data were corrected for atmospheric pressure plus the ocean's equilibrium response to pressure, and if the ocean's equilibrium response to pressure was removed from the altimeter measurements. Atmospheric pressure errors would still affect the conclusions of these studies in this case, since they would now show up in the corrected altimeter measurements. The advantage, though, is that this approach would probably be more consistent with the available data. GRACE results will most likely be provided to the user with the combined effects of atmospheric pressure and the ocean's response to pressure already removed. And altimeter data records routinely include, as a separate entry, estimated corrections for the ocean's response to pressure.

Acknowledgments.
We thank Dazhong Han for providing his elastic Love numbers and viscoelastic Green's functions and for his permission to tabulate numerical results for the elastic Green's functions; Jae Schemm and Huug van den Dool for providing us with their global, gridded, soil moisture data set; Mike Watkins, Brooks Thomas, and Srinivas Bettadpur for providing us with their estimates of the GRACE gravity field errors and for discussions of the GRACE error budget, Dailin Wang for assistance in carrying out the simulations with the POP ocean model; and Ben Chao, Pascal Gegout, and an anonymous referee for their reviews of this manuscript. This work was partially supported by NASA grant NAG5-3143 and JPL contract 958126 to the University of Colorado, by NASA grant NAG5-6549 to NCAR, and by the National Science Foundation through its sponsorship of NCAR.

References

Andersen, O.B., P.L. Woodworth, and R.A. Flather, Intercomparison of recent ocean tide models, *J. Geophys. Res., 100,* 25,249-25,259, 1995.

Barnier, B., L. Siefridt, and P. Marchesiello, Thermal forcing for a global ocean circulation model using a three-year climatology of ECMWF analysis, *J. Mar. Syst., 6,* 363-380.i, 1995.

Bryan, K., and M.D. Cox, An approximate equation of state for numerical models of ocean circulation, *J. Phys. Oceanogr., 2*(4), 510-514, 1975.

Chao, B.F., The geoid and Earth rotation, in *Geoid and Its Geophysical Interpretations,* edited by P. Vanicek and N. Christou, pp. 285-298, CRC Press, Boca Raton, Fla., 1994.

Chao, B.F., and R.S. Gross, Changes in the Earth's rotation and low-degree gravitational field induced by earthquakes, *Geophys. J. R. Astron. Soc., 91,* 569-596, 1987.

Chao, Y., and L.-L. Fu, A comparison between the TOPEX/POSEIDON data and a global ocean general circulation model during 1992-1993, *J. Geophys. Res., 100,* 24,965-24,976, 1995.

Cheng, M., R. Eanes, C. Shum, B. Schutz, and B. Tapley, Temporal variations in low degree zonal harmonics from Starlette orbit analysis, *Geophys. Res. Lett., 16,* 393-396, 1989.

Cooper, M., and K. Haines, Altimetric assimilation with water property conservation, *J. Geophys. Res., 101,* 1059-1077, 1996.

Coughlan, M., and R. Avissar, The global energy and water cycle experiment (GEWEX) continental scale international project (GCIP): An overview, *J. Geophys. Res., 101,* 7139-7147, 1996.

Dickey, J.O., et al., *Satellite Gravity and the Geosphere, National Research Council Report,* 112 pp., Nat. Acad. Washington, D.C., 1997.

Dong, D., R.S. Gross, and J.O. Dickey, Seasonal variations of the Earth's gravitational field: An analysis of atmospheric and oceanic tidal excitation, *Geophys. Res. Lett., 23,* 725-728, 1996.

Dukowicz, J., Steric sea level in the Los Alamos POP code - Non-Boussinesq effects, in *Numerical Methods in Atmospheric and Oceanic Modelling. The Andre Robert Memorial Volume,* edited by C.A. Lin, R. Laprise, and H. Ritchie, pp. 533-546, Can. Meteorol. and Oceanographics Soc. Ottawa, Ont., 1997.

Dukowicz, J.K., and R.D. Smith, Implicit free-surface method for the Bryan-Cox-Semtner ocean model, *J. Geophys. Res., 99,* 7991-8014, 1994.

Dziewonski, A., and D.L. Anderson, Preliminary reference Earth model, *Phys. Earth Planet. Inter., 25,* 297-356, 1981.

Eanes, R.J., A study of temporal variations in Earth's gravitational field using LAGEOS-1 laser ranging observations, *Ph.D. thesis, 128 pp., Univ. of Tex., Austin,* 1995

Farrell, W.E., Deformation of the Earth by surface loading, *Rev. Geophys., 10,* 761-797, 1972.

Fu, L , and R.D. Smith, Global ocean circulation from satellite altimetry and high-resolution computer simulation, *Bull. Am. Meteorol. Soc., 77,* 2625-2636, 1996.

Gegout, P., and A. Cazenave, Temporal variations of the Earth gravity field for 1985-1989 derived from LAGEOS, *Geophys. J. Int., 114,* 347-359, 1993.

Gill, A.E., and P.P. Niiler, The theory of seasonal variability in the ocean, *Deep Sea Res., 20,* 141-177, 1973.

Greatbatch, R.J., A note on the representation of steric sea level in models that conserve volume rather than mass, *J. Geophys. Res., 99,* 12,767-12,771, 1994.

Han, D., and J. Wahr, The viscoelastic relaxation of a realistically stratified Earth, and a further analysis of postglacial rebound, *Geophys. J. Int., 120,* 287-311, 1995.

Huang. J., H. van den Dool, and K.P. Georgakakos, Analysis of model-calculated soil moisture over the United States

(1931-1993) and application to long-range temperature forecasts, *J. Clim., 9*, 1350-1362, 1996.

Jekeli, C., Alternative methods to smooth the Earth's gravity field, *Rep. 327*, Dep. of Geod. Sci. and Surv., Ohio State Univ., Columbus, 1981.

Levitus, S., R. Burgett, and T. Boyer, *World Ocean Atlas 1994*, vol. 3, *Salinity*, U.S. Dep. of Commer., Washington, D. C., 1994.

Nerem, R.S., B.F.Chao, A.Y. Au, J.C. Chan, S.M. Klosko, N.K. Pavlis, and R.G. Williamson, Time variations of the Earth's gravitational field from satellite laser ranging to Lageos, *Geophys. Res. Lett., 20*, 595-598, 1993.

Peltier, W.R., Ice age paleotopography, *Science, 265*, 195-201, 1994.

Ponte, R.M., Variability in a homogeneous global ocean forced by barometric pressure, *Dyn. Atmos. Oceans., 18*, 209-234, 1993.

Rubincam, D.P., Postglacial rebound observed by Lageos and the effective viscosity of the lower mantle, *J. Geophys. Res., 89*, 1077-1088, 1984.

Smith, R.D., S. Kortas, and B. Melts, Curvilinear coordinates for global ocean models, *Los Alamos Nat. Lab. Tech. Rep., LA-UR-95-1146*, 1995.

Tapley, B.D., et al., The joint gravity field model 3, *J. Geophys. Res., 101*, 28,029-28,049, 1996.

Trenberth, K.E., and C.J. Guillemot, The total mass of the atmosphere, *J. Geophys. Res., 99*, 23,079-23,088, 1994.

Trupin, A.S., M.F. Meier, and J.M. Wahr, The effect of melting glaciers on the Earth's rotation and gravitational field: 1965-1984, *Geophys. J. Int., 108*, 1-15, 1992.

Tushingham A.M., and W.R. Peltier, Ice-3G: A new global model of late pleistocene deglaciation based upon geophysical predictions of postglacial relative sea level change *J. Geophys. Res., 96*, 4497-4523, 1991.

vanDam, T.M., J. Wahr, Y. Chao, and E. Leuliette, Predictions of crustal deformation and of geoid and sea level variability caused by oceanic and atmospheric loading, *Geophys. J. Int., 129*, 507-517, 1997.

Wahr, J.M., and Z. Bergen, The effects of mantle anelasticity on nutations, Earth tides, and tidal variations in rotation rate, *Geophys. J. R. Astron. Soc., 87*, 633-668, 1986.

Wunsch, C., and D. Stammer, Atmospheric loading and the oceanic "inverted barometer" effect. *Rev. Geophys., 35*, 79-107, 1997.

Yoder, C.F., J.G. Williams, J.O. Dickey, B.E. Schutz, R.J. Eanes, and B.D. Tapley, Secular variations of Earth's gravitational harmonic *Jsub*2 coefficient from Lageos and the non-tidal acceleration of Earth rotation, *Nature, 303*, 757-762, 1983.

F. Bryan, NCAR, P.O. Box 3000, Boulder, CO 80307-3000 (e-mail: bryan@cgd.ucar.edu)

M. Molenaar and J. Wahr, Department of Physics, University of Colorado, Campus Box 390, Boulder, CO 80309-0390 (e-mail: wahr@lemond.Colorado.edu)

(Received April 8, 1998; revised July 29, 1998; accepted August 25, 1998.)